Centrum Wiskunde & Informatica

Simultaneous Tomographic Image Reconstruction and Motion Estimation

Felix Lucka

UGCT Seminar
22 February 2021

Example: In Vivo Time-Resolved Microtomography

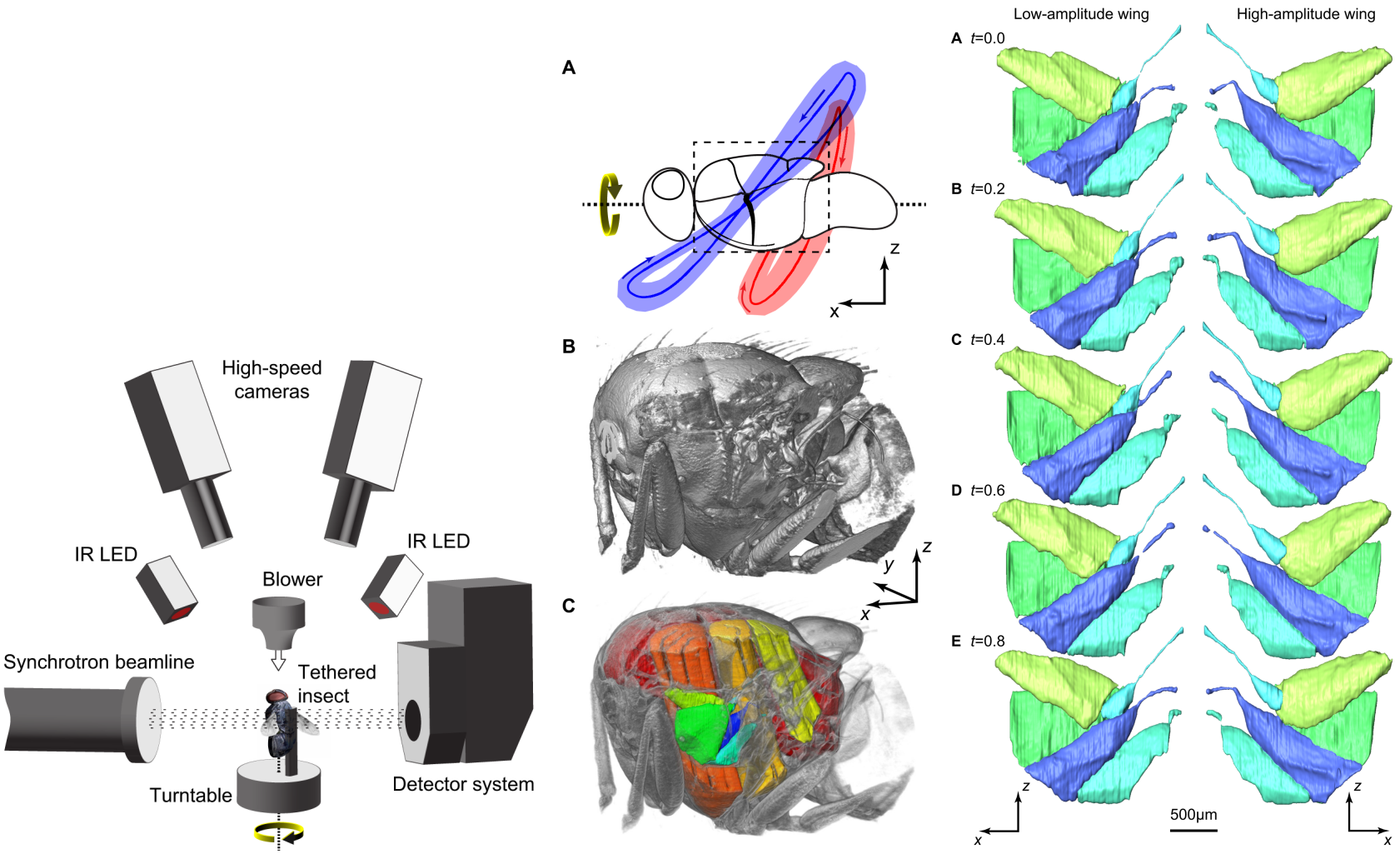

Walker, Schwyn, Mokso, Wicklein, Müller, 2014. In Vivo Time-Resolved Microtomography Reveals the Mechanics of the Blowfly Flight Motor, *PLoS Biol 12(3).*

Example: Fluidized Bed Reactors

Collaboration with the Transport Phenomena group at TU Delft.

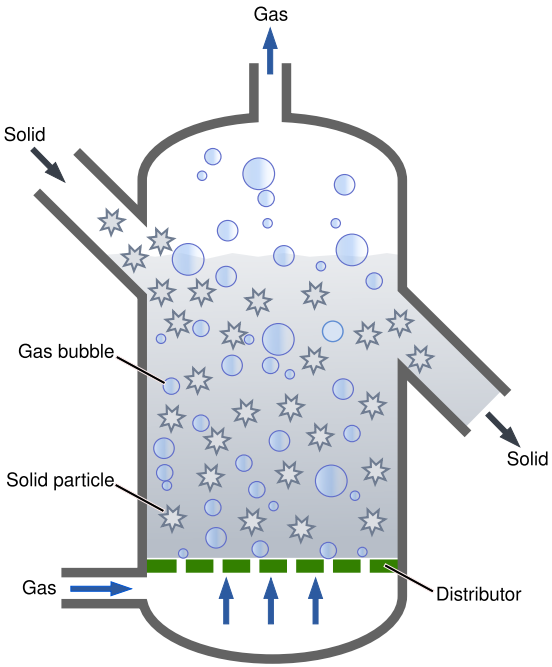

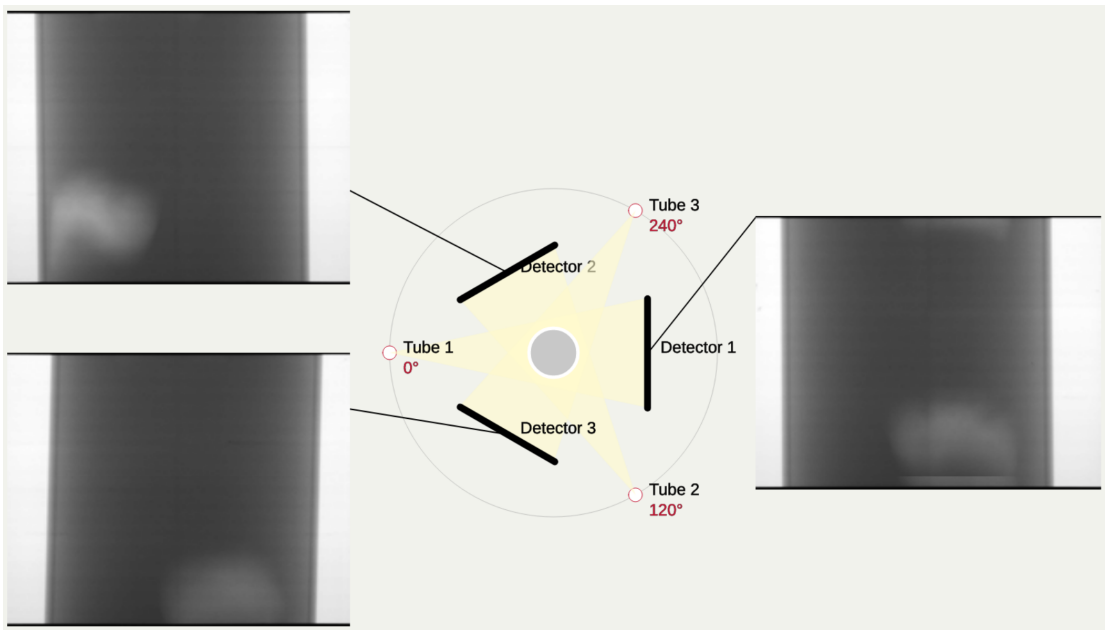

Own Experiments: Two-Phase Flow Instability

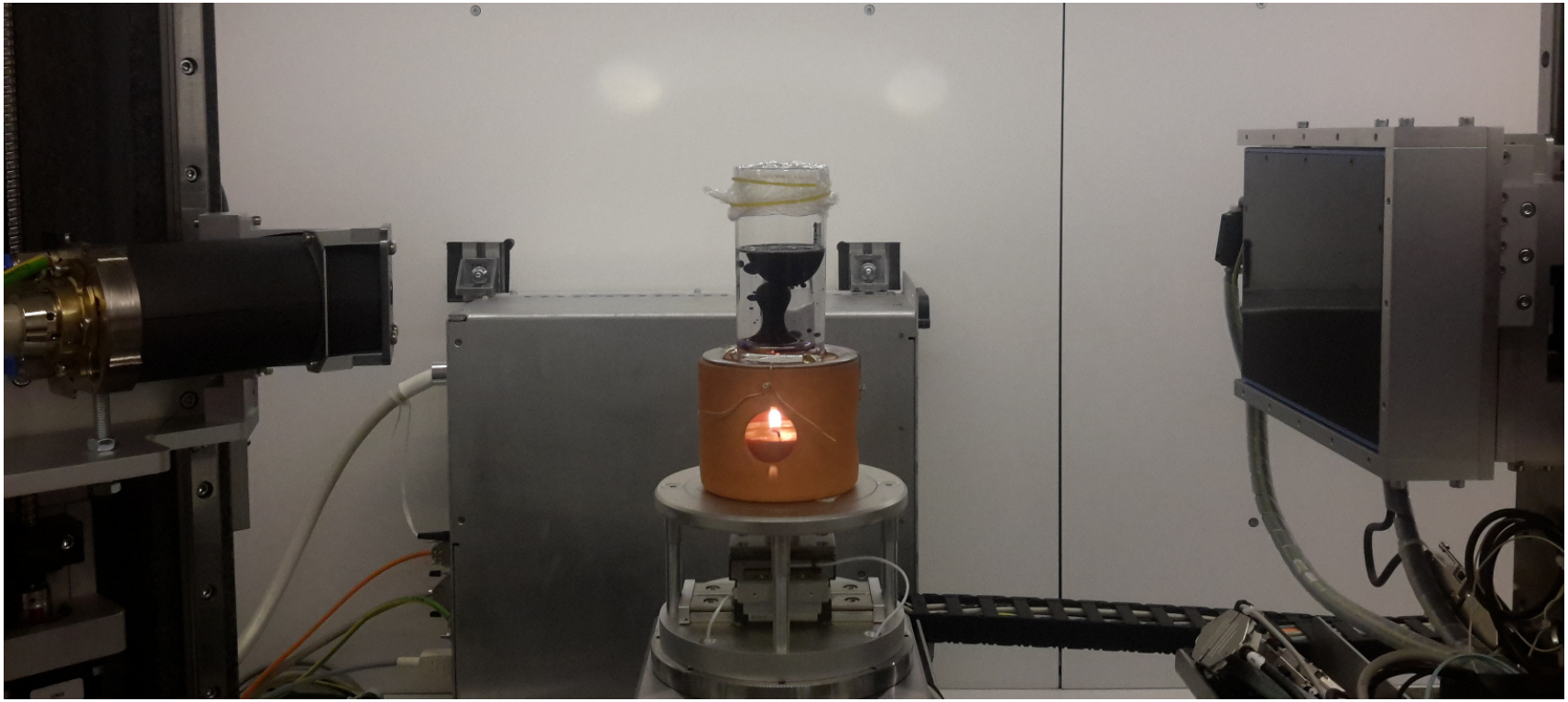

- canonical example of temperature-driven **two-phase flow instability**
- 120 projections per rotation $\rightarrow$ each projection averaged over 3°
- 40ms exposure per projection $\rightarrow$ 4.8s per rotation

Own Experiments: Two-Phase Flow Instability

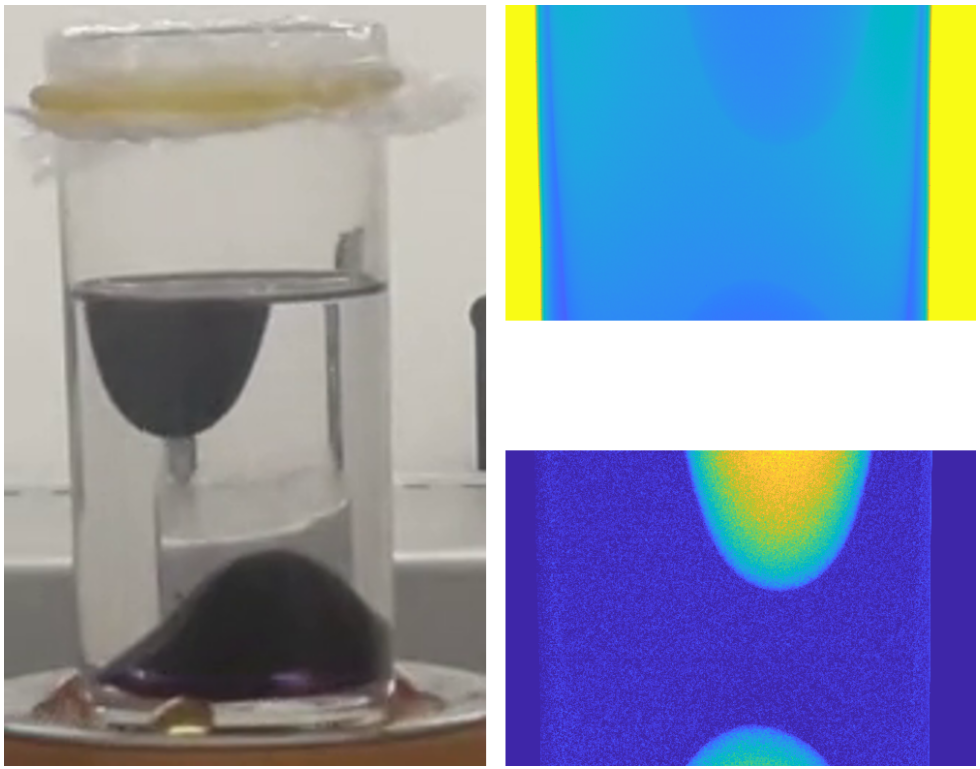

- canonical example of temperature-driven **two-phase flow instability**
- 120 projections per rotation $\rightarrow$ each projection averaged over 3°
- 40ms exposure per projection $\rightarrow$ 4.8s per rotation

Overview Dynamic Imaging

Applications

- scientific, industrial and clinical
- vast range of dynamics (rigid motion, elastic deformation, fluid dynamics, crack formation, chemical kinetics, granular flows, ...)

Goals

- motion compensation
- full dynamic reconstruction (+ simultanous motion estimation?)
- retrospective / real time / prediction
- parameter identification in dynamical systems

Challenges

- no high quality frame-by-frame reconstruction possible (motion artefacts, no gating, noise, low angular res,...)
- mathematical modeling of dynamics
- computational image reconstruction

Sequential Image Reconstruction and Correspondence Analysis

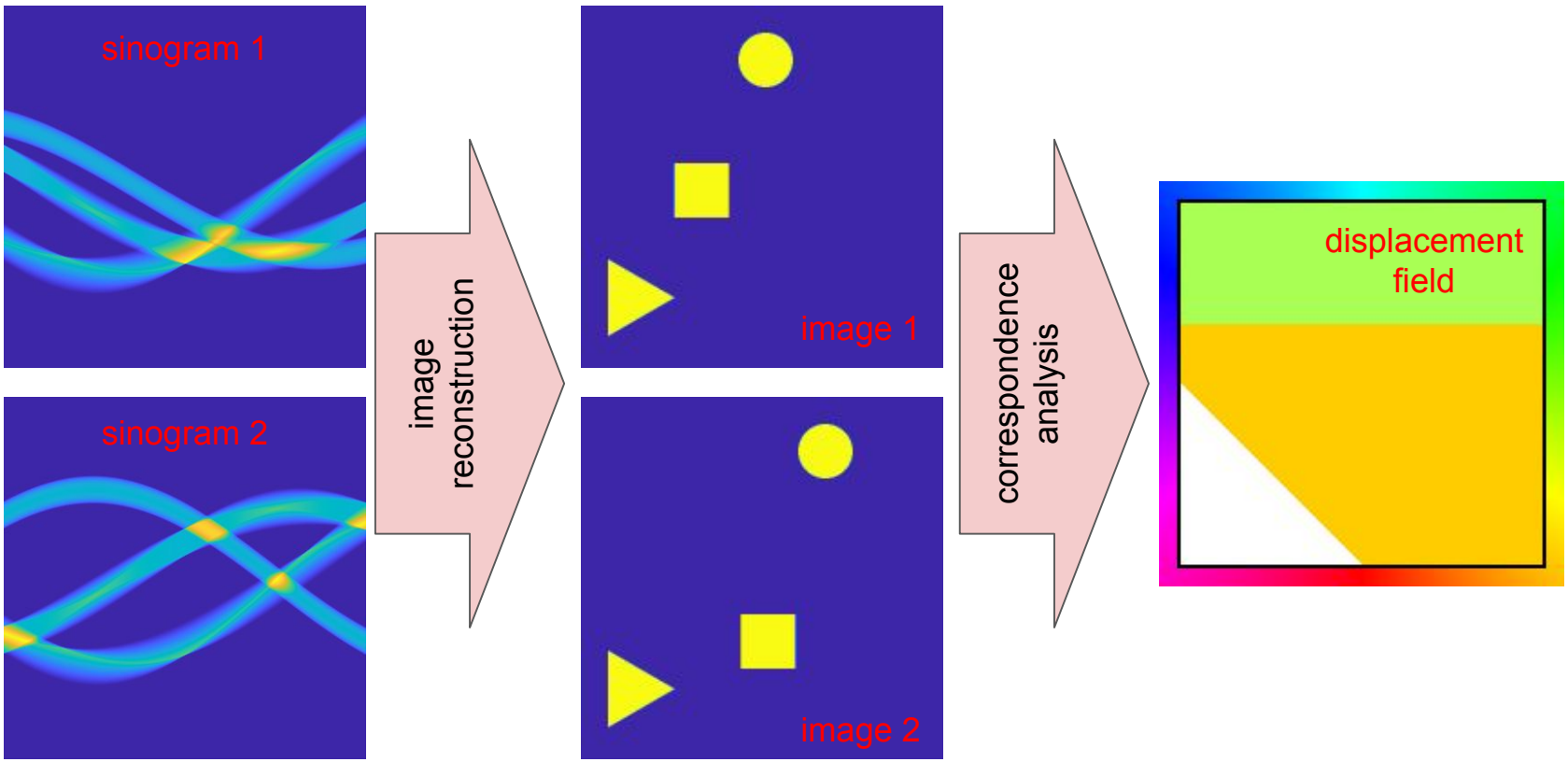

Alternating Image Reconstruction and Correspondence Analysis

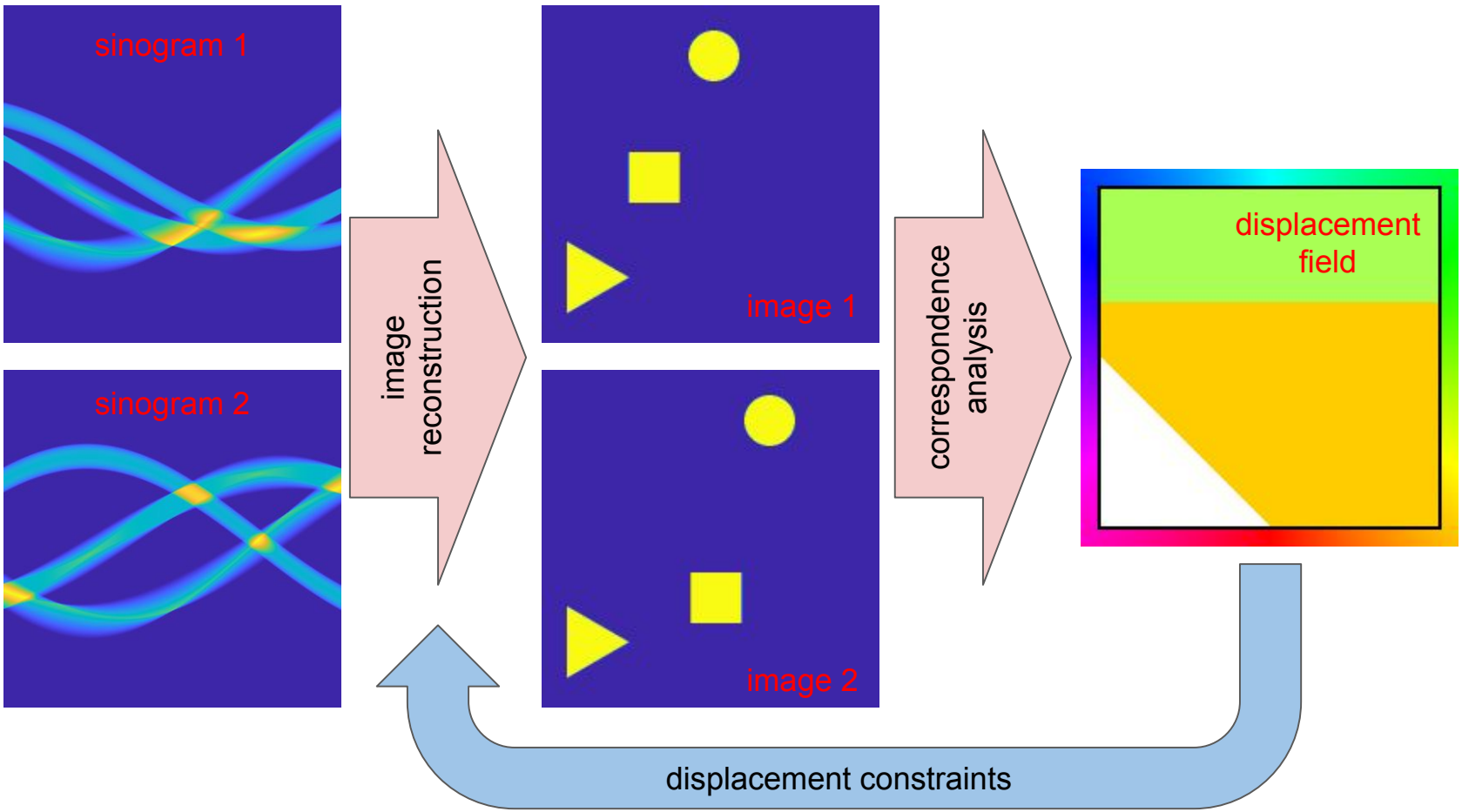

Overview Mathematical Setup and Challenges

static

$$f = Au^{\dagger}$$

dynamic

$$f(t) = C(t)Au^{\dagger}(t)$$

binned

$$\underbrace{\begin{bmatrix} f(t_i) \\ \vdots \\ f(t_j) \end{bmatrix}}_{f_{ij}} = \underbrace{\begin{bmatrix} C(t_i) \\ \vdots \\ C(t_j) \end{bmatrix}}_{C_{ij}} Au_{ij}$$

✓ static reconstruction of sufficient quality

! $C(t)$ reduces dimension of data

! trade-off:

- larger bins $\longrightarrow$ more motion-blur
- smaller bins $\longrightarrow$ more underdetermined (limited-angle)

! sequential scanning is worst sub-sampling ($\neq$ "compressed sensing")

! high computational/memory demands

Illustration: Limited-View Artifacts

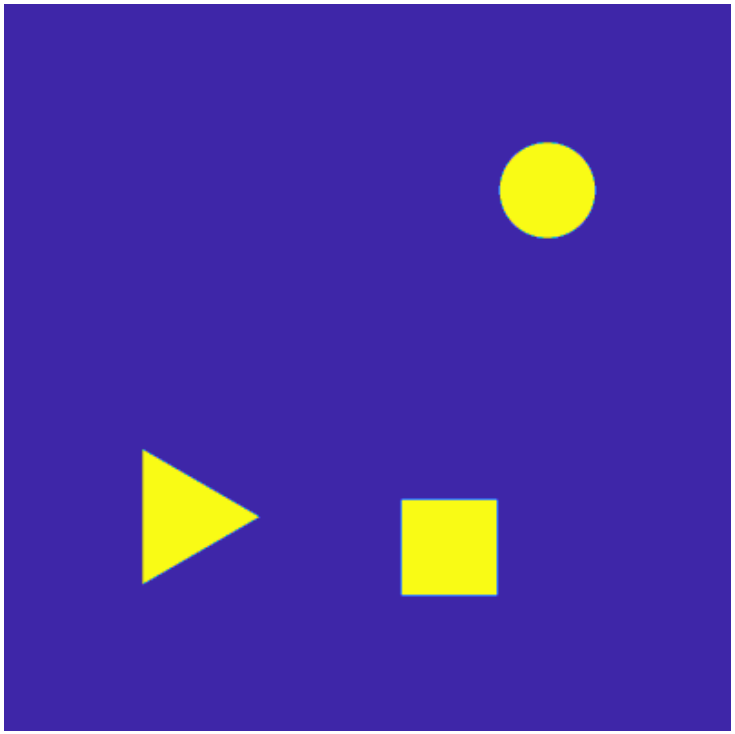

true image $u^\dagger$

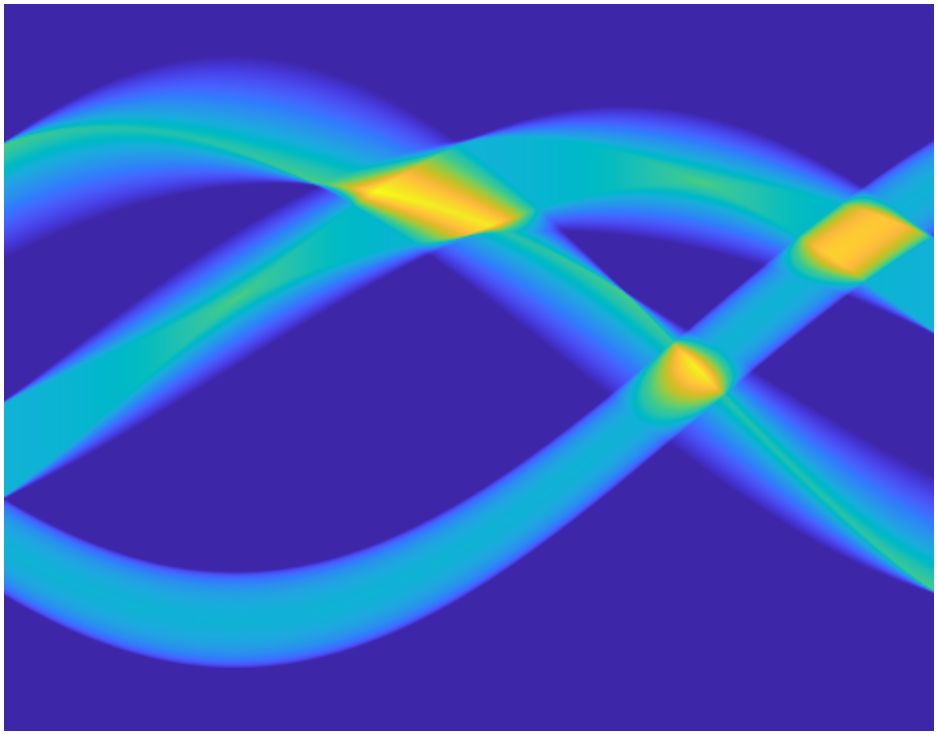

sinogram $Au^\dagger$

Illustration: Limited-View Artifacts

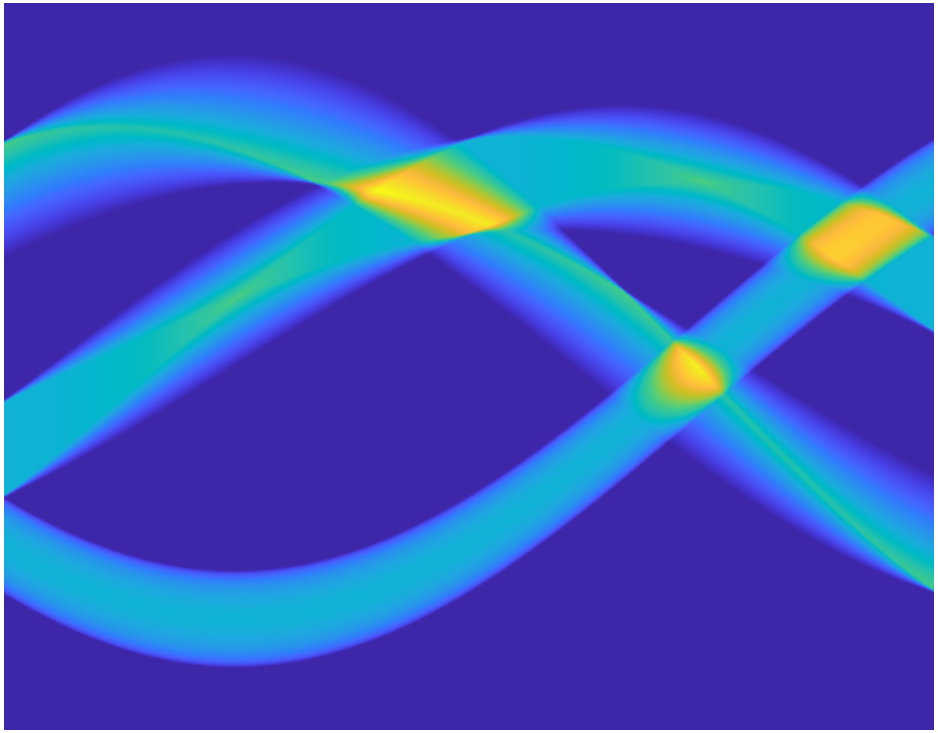

sinogram f

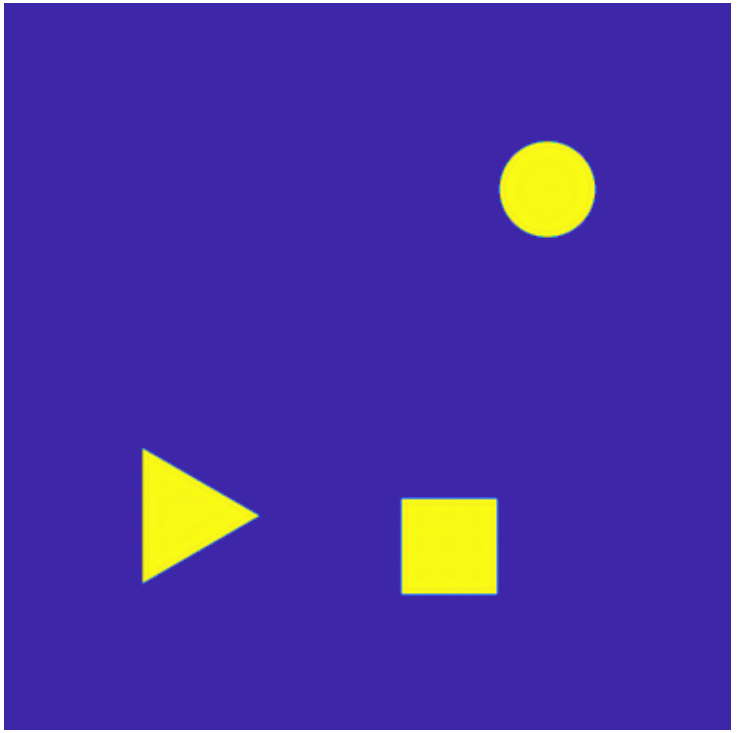

reconstruction $\hat{u}$

accelerated gradient descent to solve

$$\hat{u} = \operatorname*{argmin}_{u \geq 0} \ \|Au - f\|_2^2$$

Illustration: Total Variation in Space and Time

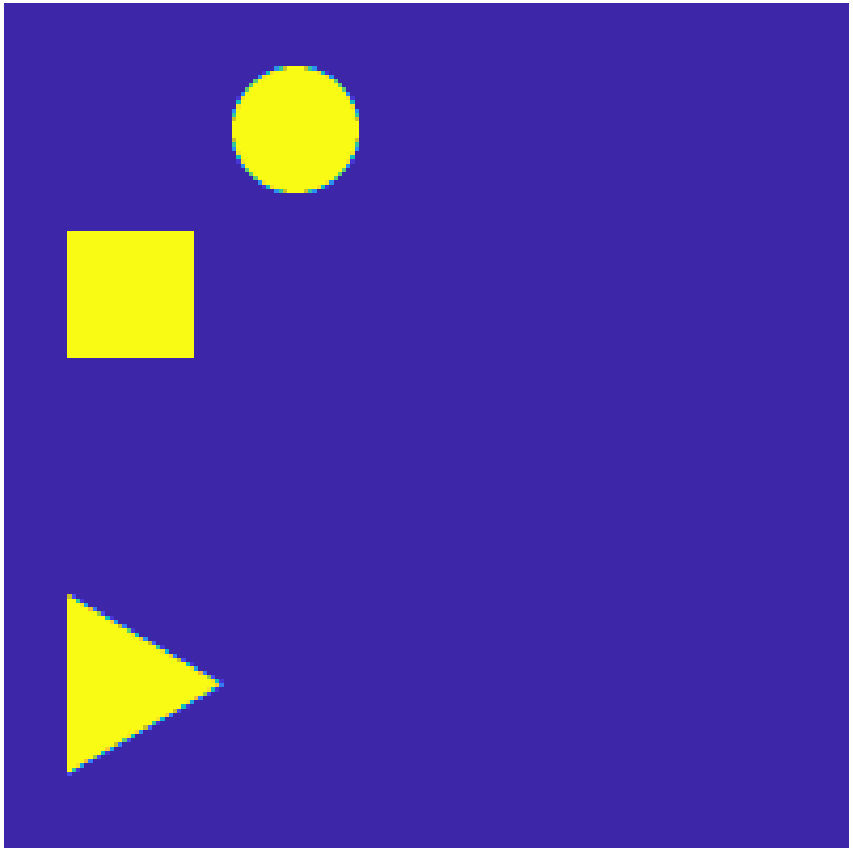

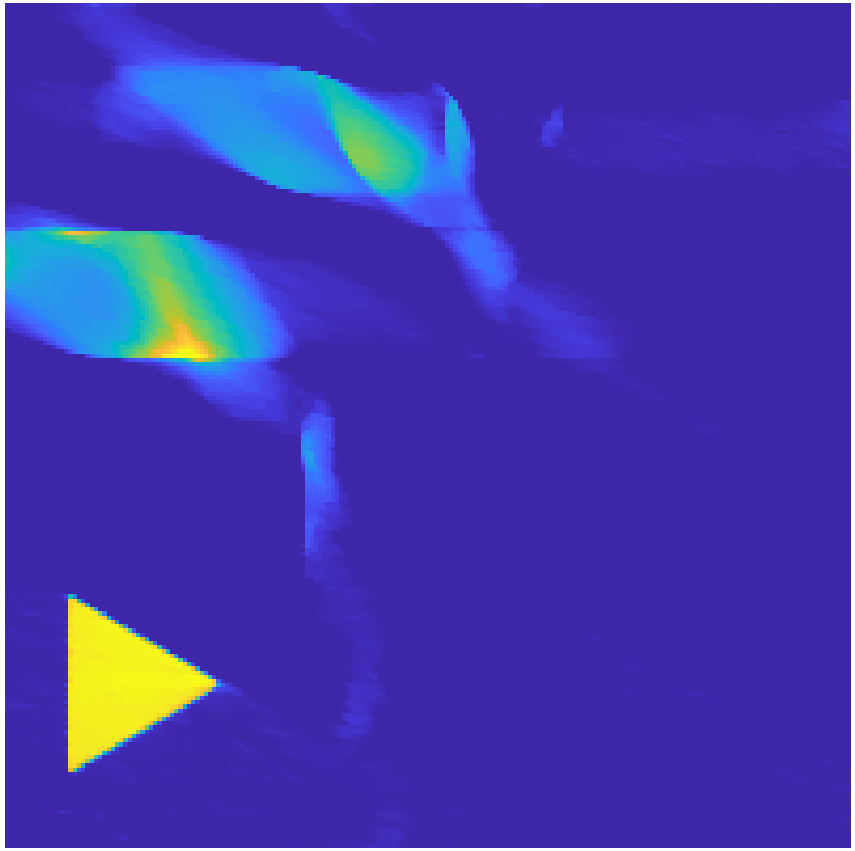

large γ

$$\hat{u} = \underset{u \geqslant 0}{\operatorname{argmin}} \ \frac{1}{2} \sum_i \|C_i A u_i - f_i\|_2^2 + \alpha \|\nabla u_i\|_1 + \gamma^2/2 \, \|u_i - u_{i-1}\|_2^2$$

Illustration: Total Variation in Space and Time

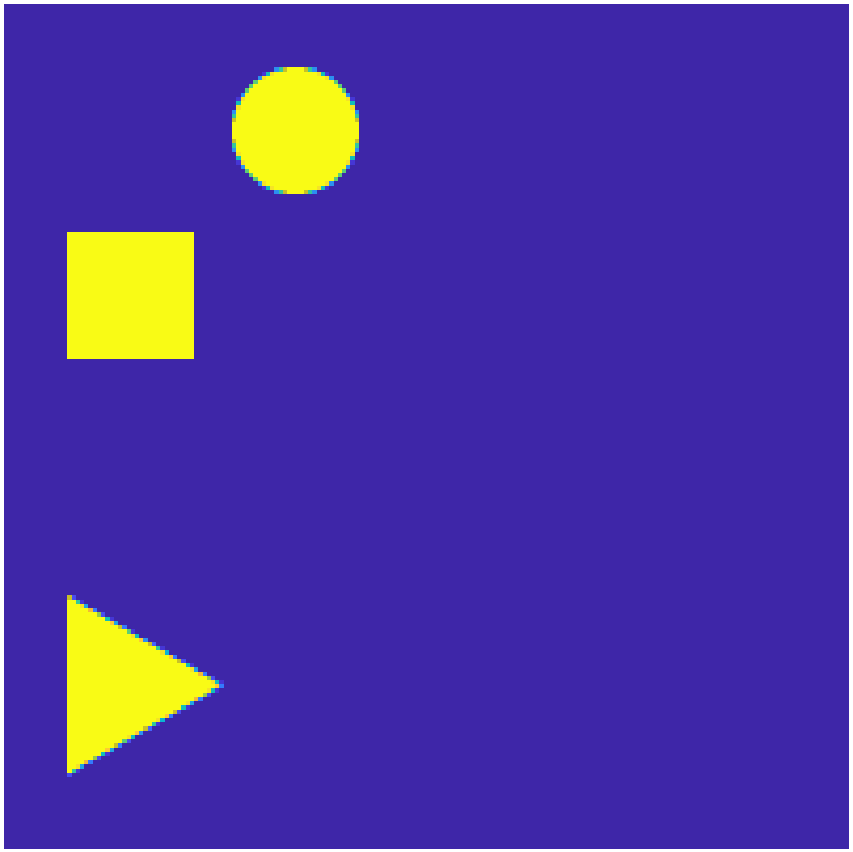

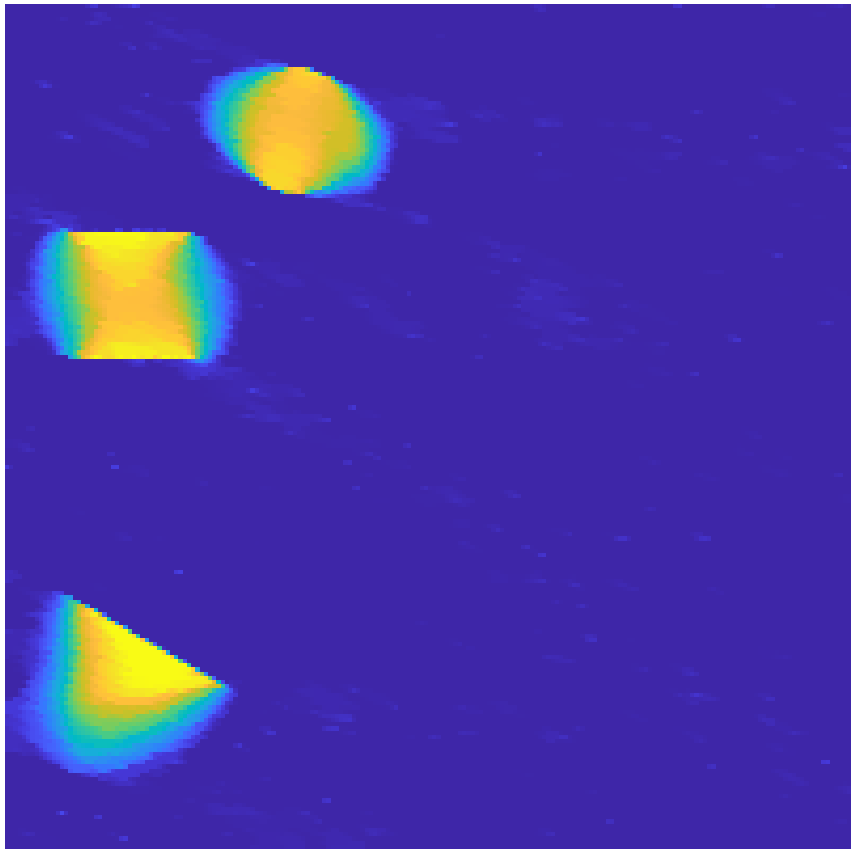

small γ

$$\hat{u} = \underset{u \geqslant 0}{\operatorname{argmin}} \ \tfrac{1}{2} \sum_i \|C_i A u_i - f_i\|_2^2 + \alpha \|\nabla u_i\|_1 + \gamma^2/2 \, \|u_i - u_{i-1}\|_2^2$$

Illustration: Total Variation in Space and Time

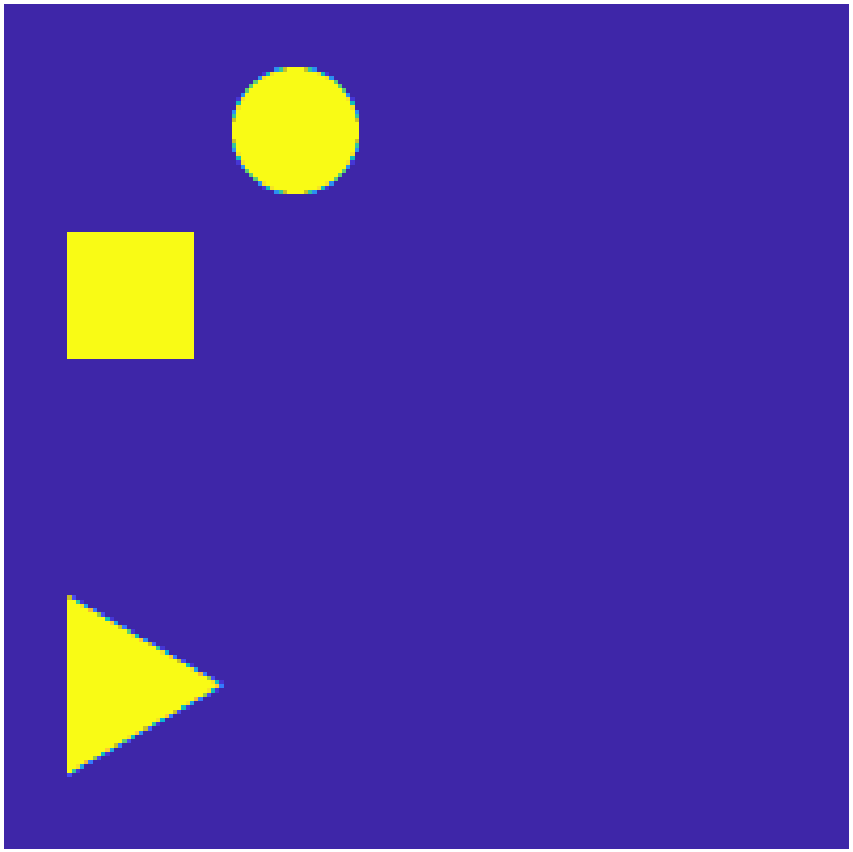

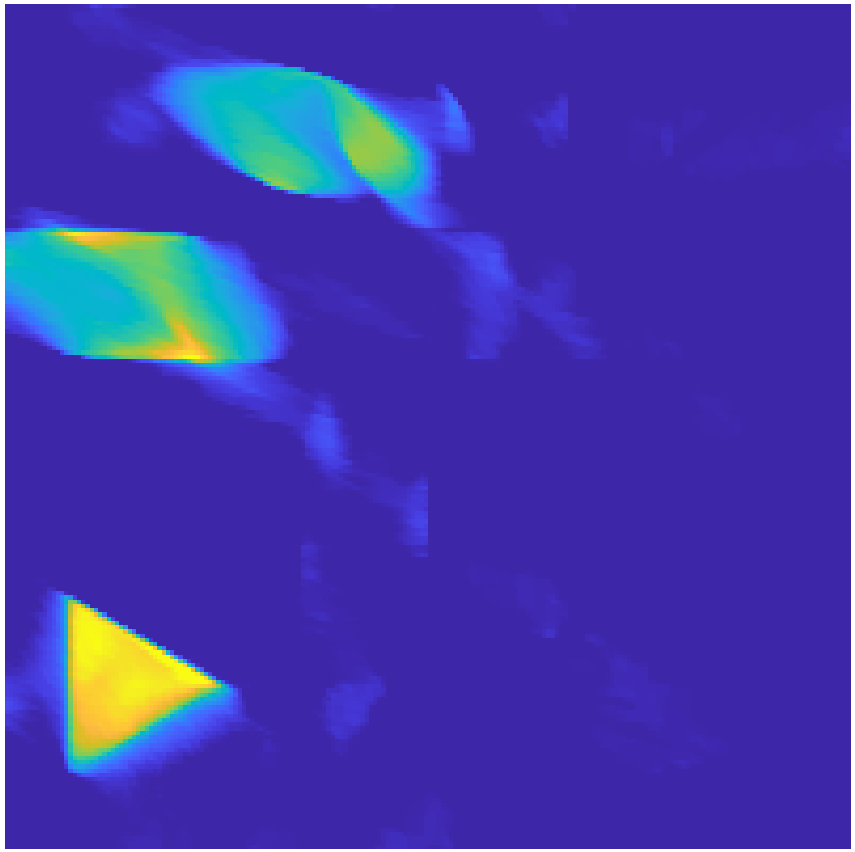

large γ

$$\hat{u} = \underset{u \geqslant 0}{\operatorname{argmin}} \ \tfrac{1}{2} \sum_i \|C_i A u_i - f_i\|_2^2 + \alpha \|\nabla u_i\|_1 + \gamma \|u_i - u_{i-1}\|_1$$

Illustration: Total Variation in Space and Time

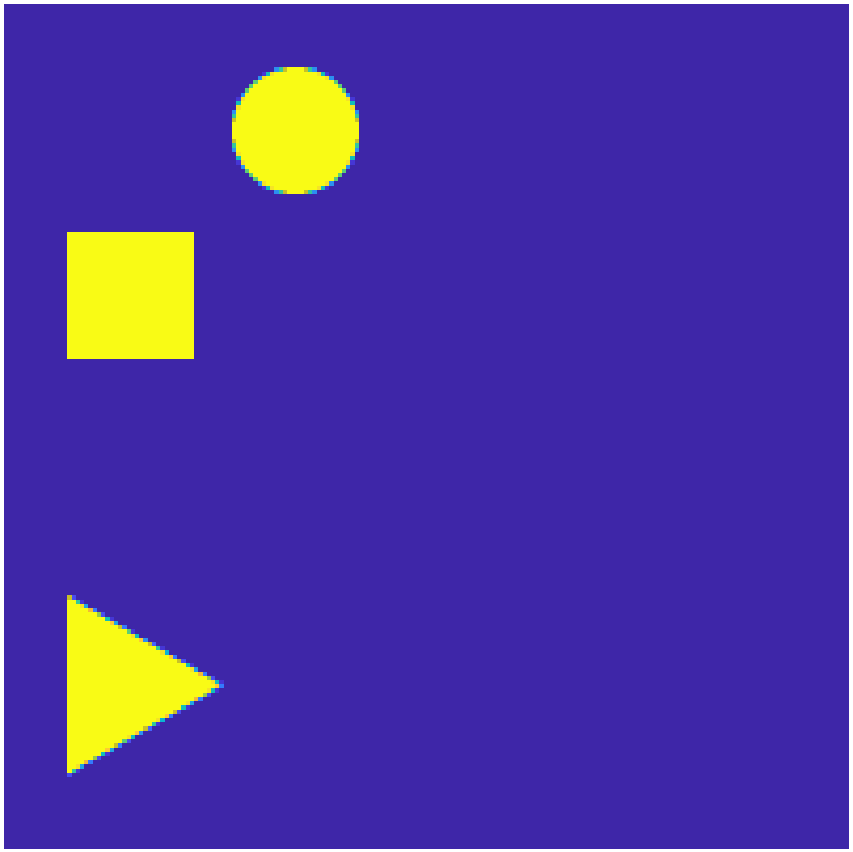

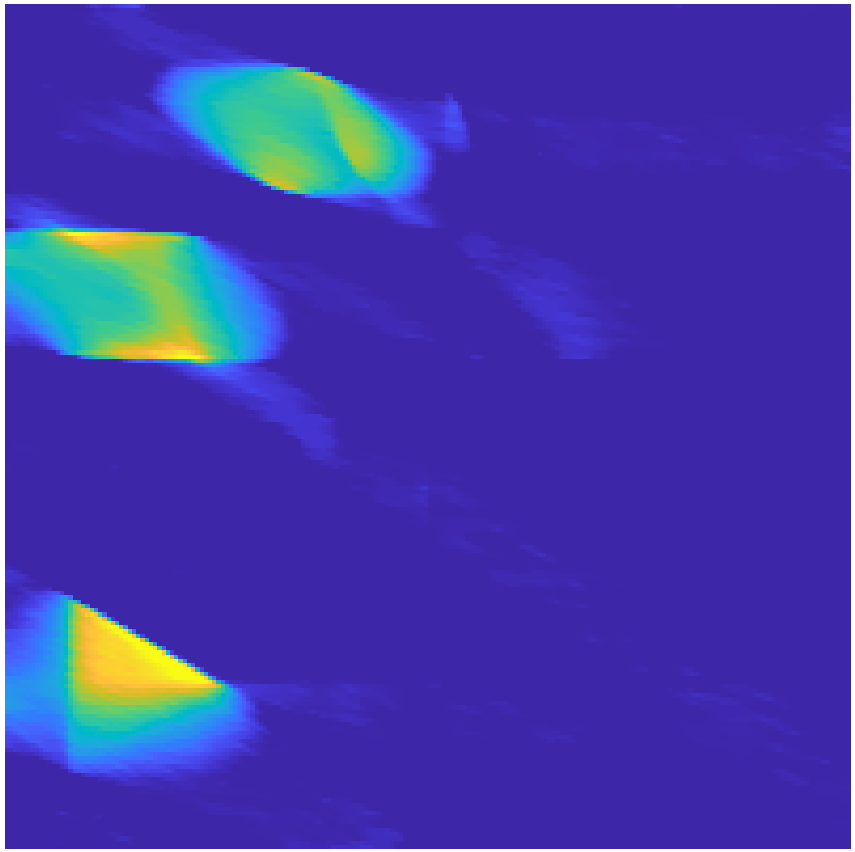

small γ

$$\hat{u} = \underset{u \geqslant 0}{\operatorname{argmin}} \ \tfrac{1}{2} \sum_i \|C_i A u_i - f_i\|_2^2 + \alpha \|\nabla u_i\|_1 + \gamma \|u_i - u_{i-1}\|_1$$

Variational Space-Time Decomposition

Implicit spatio-temporal decomposition via **infimal convolutions**:

$$\hat{u} = \underset{u \geqslant 0, w}{\operatorname{argmin}} \ \frac{1}{2} \sum_i \| C_i A u_i - f_i \|_2^2 + \alpha \, TV_{\beta_1}(u - w) + \gamma \, TV_{\beta_2}(w)$$

Holler, Kunisch, 2014. On infimal convolution of TV type functionals and applications to video and image reconstruction, *SIAM IS.*

Schloegl, Holler, Schwarzl, Bredies, Stollberger, 2017. Infimal Convolution of Total Generalized Variation Functionals for Dynamic MRI, *MAGN.*

Explicit decomposition of Casorati matrix via **low-rank + sparsity** models:

$$\hat{u} = \underset{U_l, U_S}{\operatorname{argmin}} \ \frac{1}{2} \| A(U_L + U_S) - F \|_2^2 + \alpha_L \| L U_L \|_* + \alpha_S \| S U_S \|_1$$

Ravishankar, Ye, Fessler, 2019. Image Reconstruction: From Sparsity to Data-adaptive Methods and Machine Learning, *arXiv:1904.02816.*

Illustration: Motion Artifacts

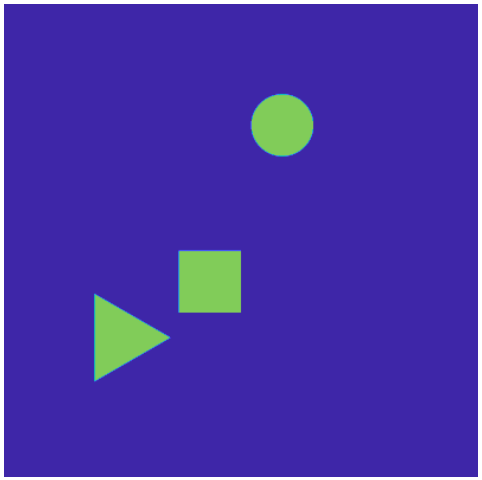

$u^\dagger$

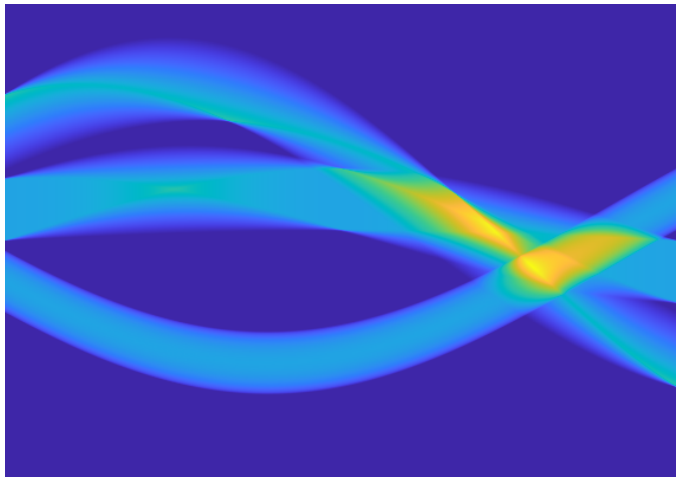

sinogram f

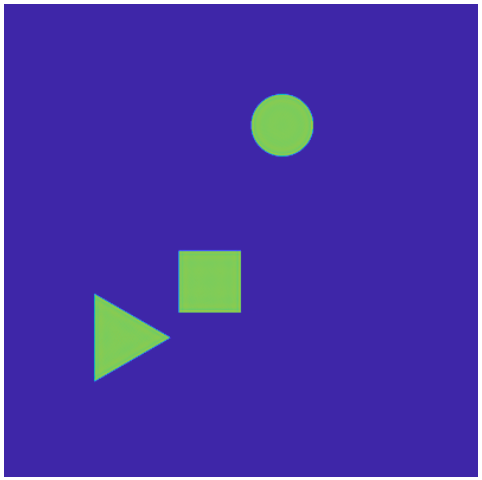

reconstruction $\hat{u}$

accelerated gradient descent to solve

$$\hat{u} = \operatorname*{argmin}_{u \geq 0} \ \|Au - f\|_2^2$$

Illustration: Motion Artifacts

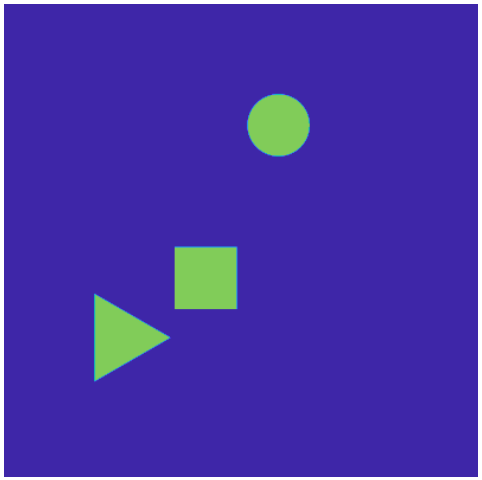

$u^\dagger$

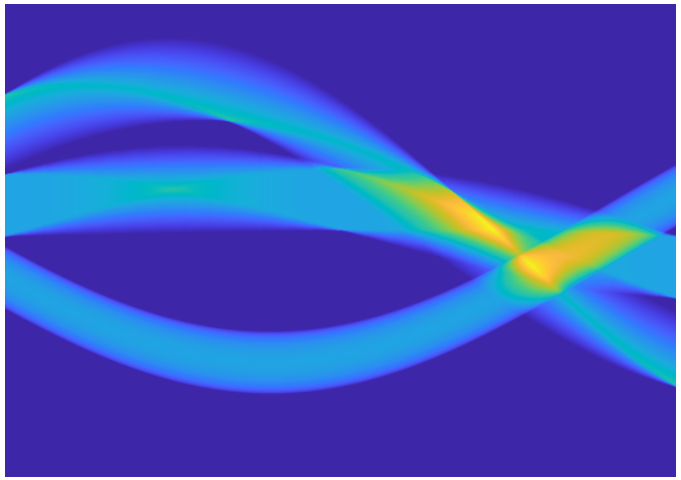

sinogram f

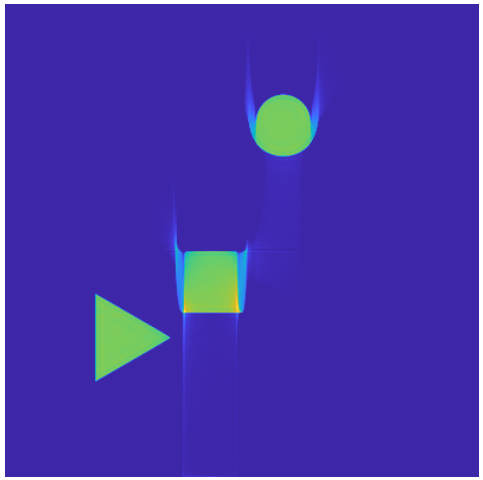

reconstruction $\hat{u}$

accelerated gradient descent to solve

$$\hat{u} = \operatorname*{argmin}_{u \geq 0} \ \|Au - f\|_2^2$$

Illustration: Motion Artifacts

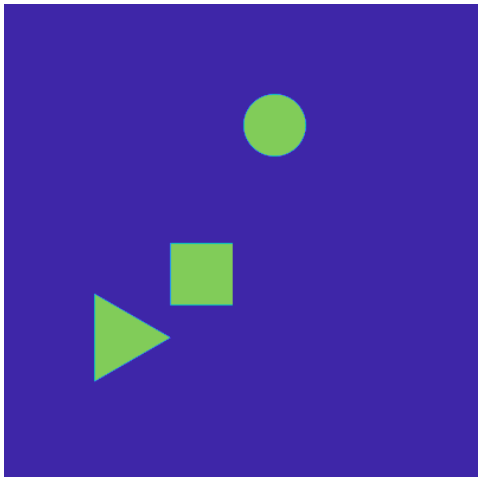

$u^\dagger$

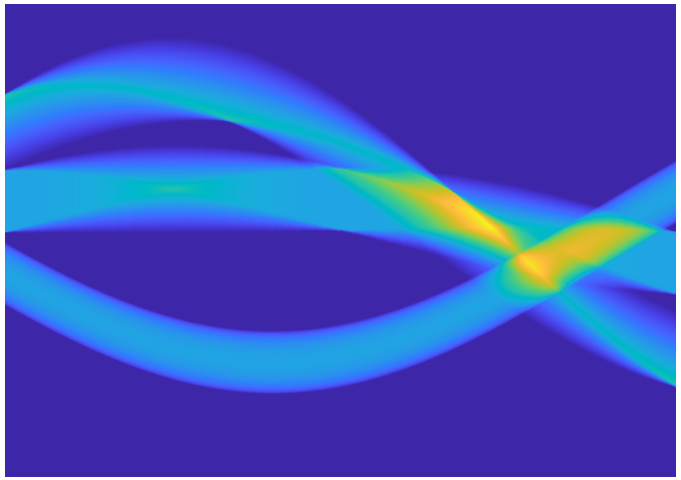

sinogram f

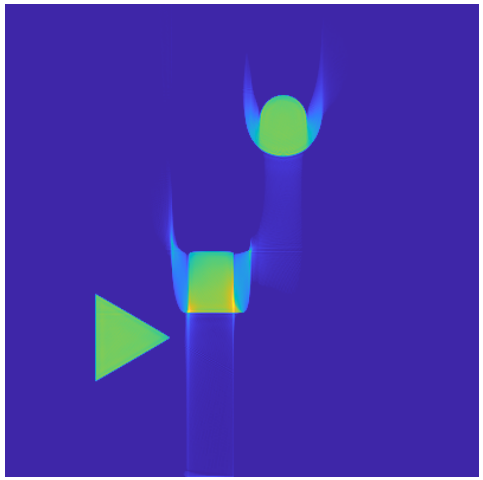

reconstruction $\hat{u}$

accelerated gradient descent to solve

$$\hat{u} = \operatorname*{argmin}_{u \geq 0} \ \|Au - f\|_2^2$$

Illustration: Motion Artifacts

$u^\dagger$

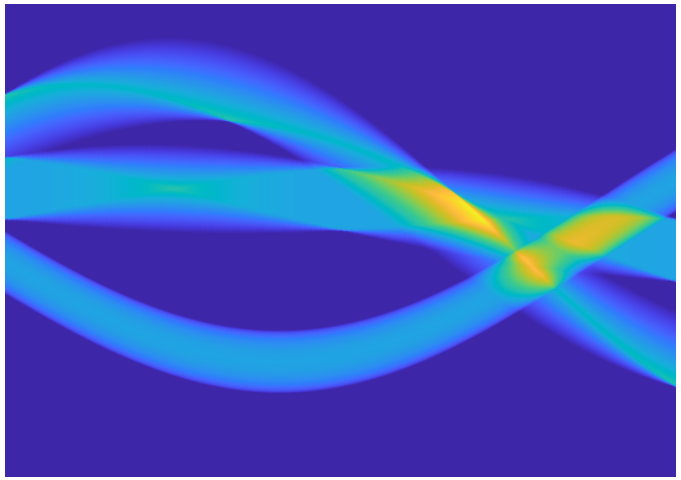

sinogram f

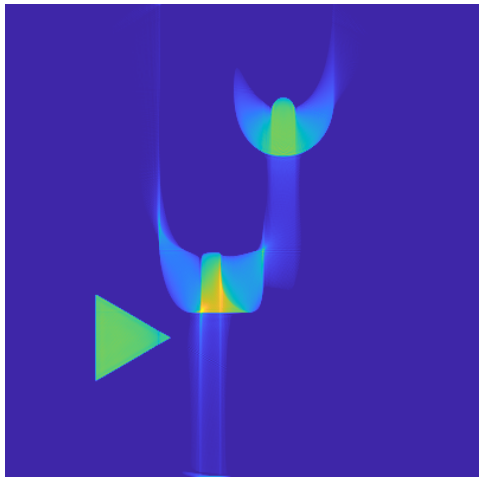

reconstruction $\hat{u}$

accelerated gradient descent to solve

$$\hat{u} = \operatorname*{argmin}_{u \geq 0} \ \|Au - f\|_2^2$$

Illustration: Motion Artifacts

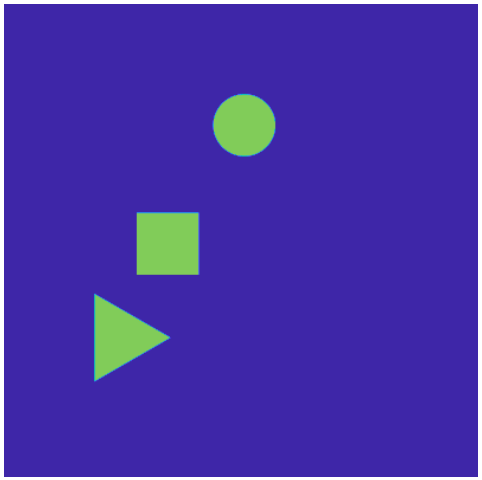

$u^\dagger$

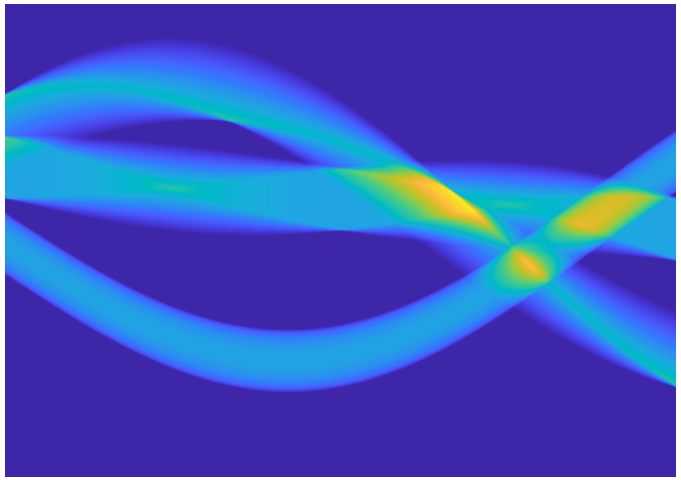

sinogram f

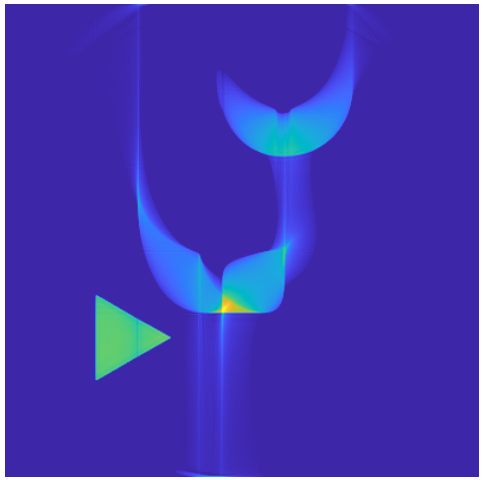

reconstruction $\hat{u}$

accelerated gradient descent to solve

$$\hat{u} = \operatorname*{argmin}_{u \geq 0} \ \|Au - f\|_2^2$$

Illustration: Motion Artifacts

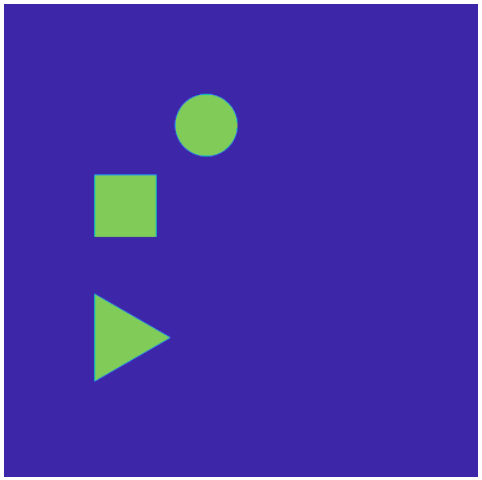

$u^\dagger$

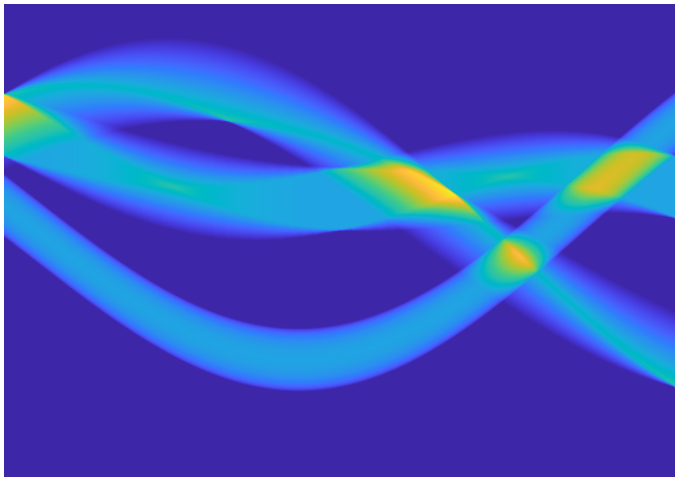

sinogram f

reconstruction $\hat{u}$

accelerated gradient descent to solve

$$\hat{u} = \operatorname*{argmin}_{u \geq 0} \ \|Au - f\|_2^2$$

Lava Lamp: Frame-by-Frame Reconstruction

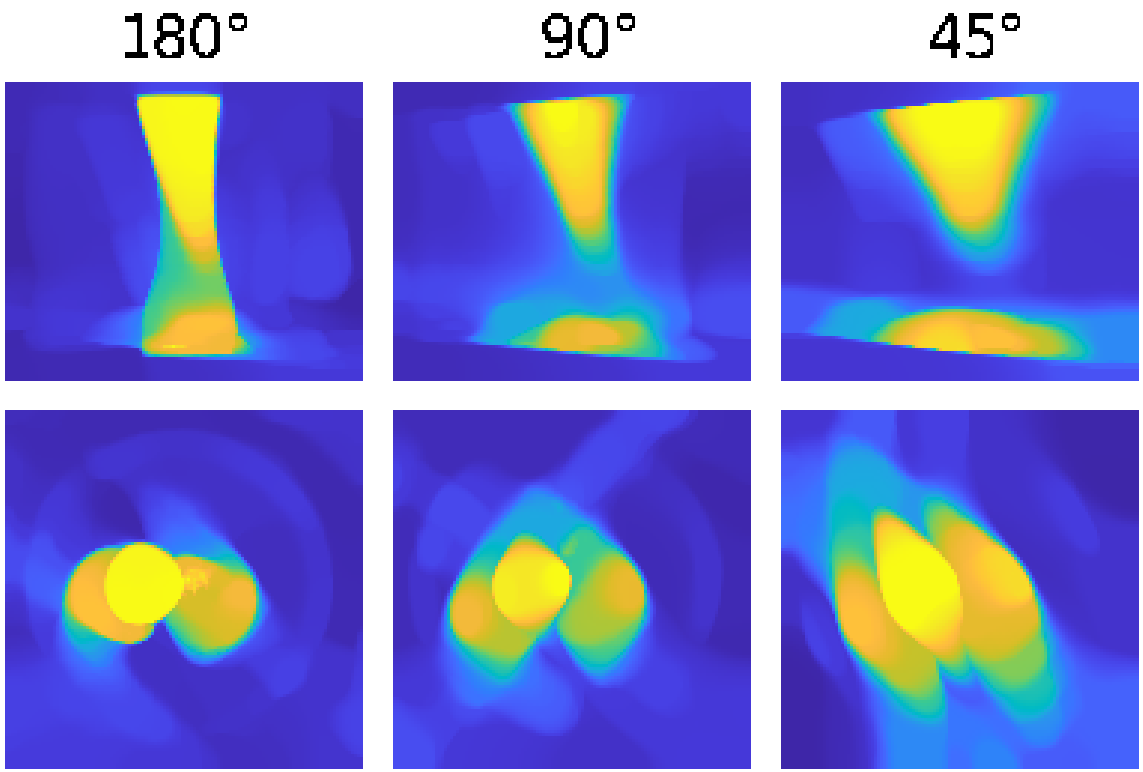

Sequential Image Reconstruction and Correspondence Analysis

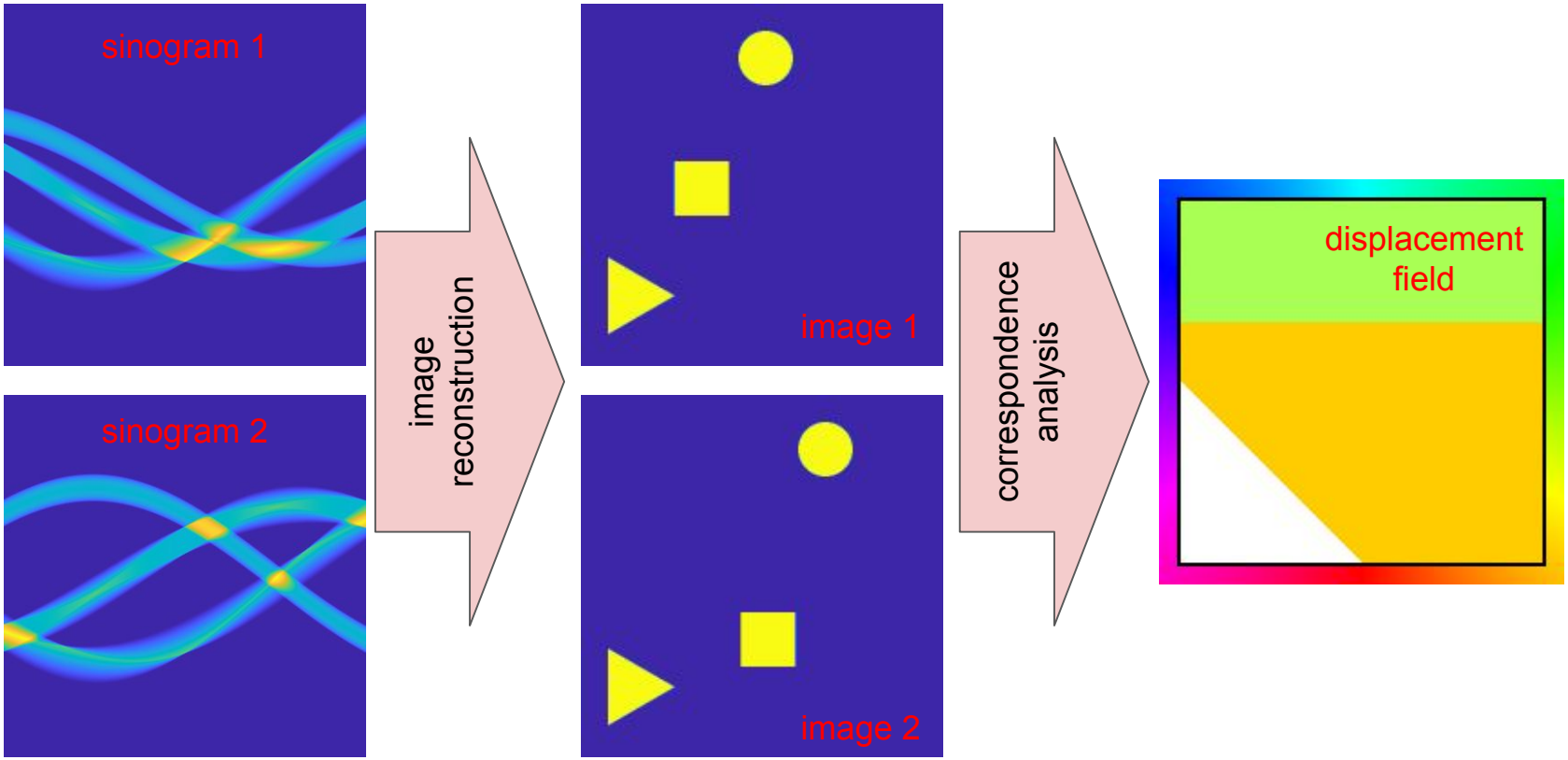

Correspondence Problems

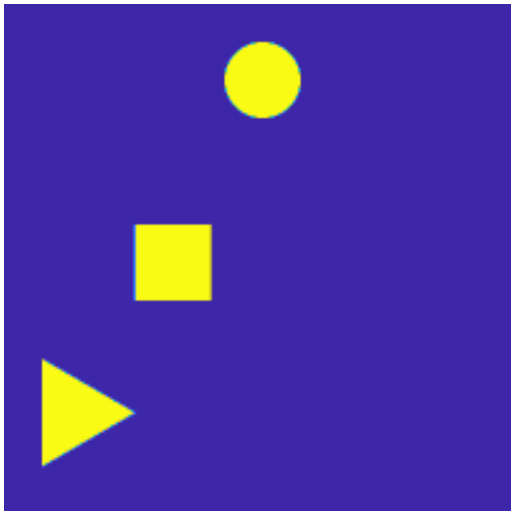

u_1

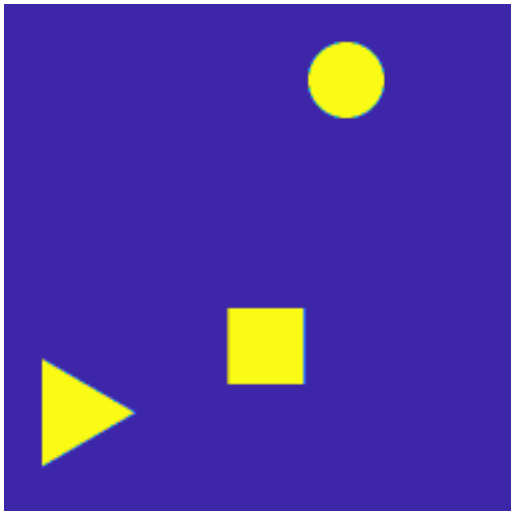

u_2

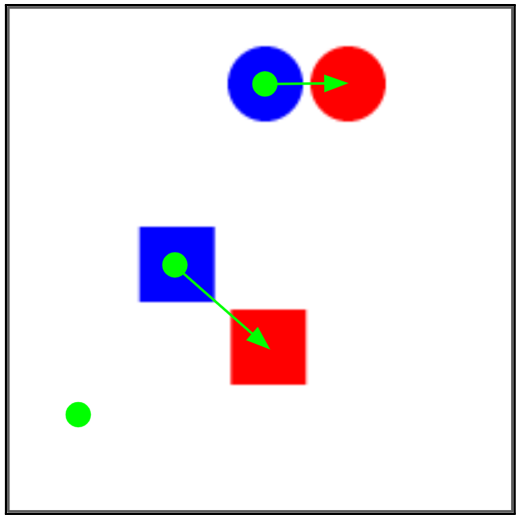

$u_2 - u_1$

search for correspondences in images taken at different times, from different perspectives and/or with different sensors

- tracking, optical flow, stereo vision, deformation
- computer vision, medical imaging, fluid dynamics
- "displacement / motion / deformation / flow / ..."

Methods: correlation based, descriptor/patch based, variational, deep learning, sparse vs. dense

Correspondence Problems

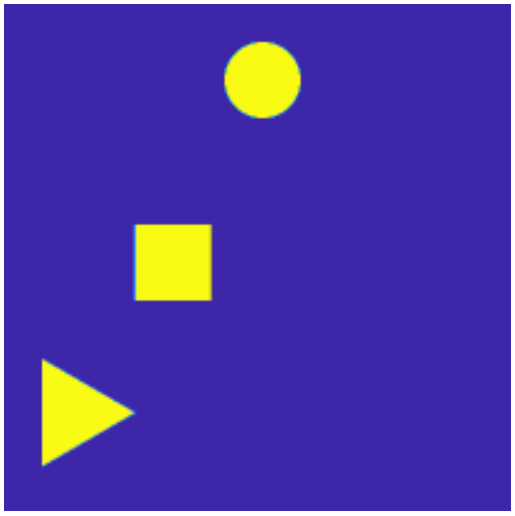

u_1

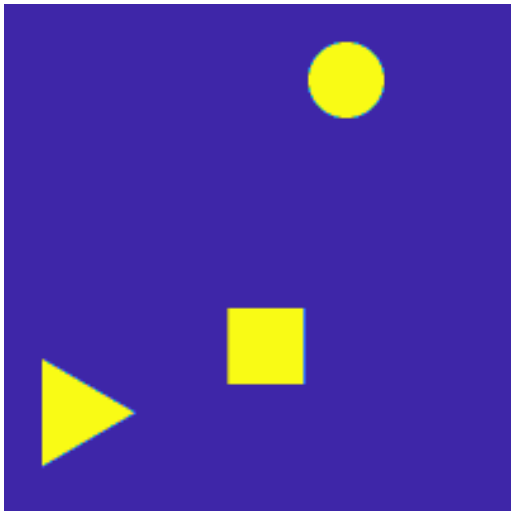

u_2

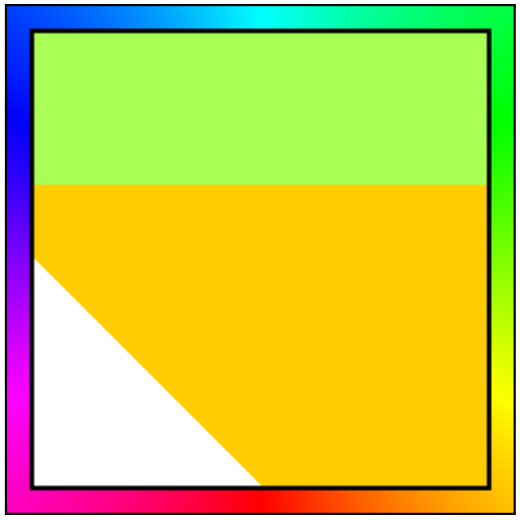

displacement

search for correspondences in images taken at different times, from different perspectives and/or with different sensors

- tracking, optical flow, stereo vision, deformation, ...
- computer vision, medical imaging, fluid dynamics, ...
- "displacement / motion / deformation / flow / ..."

Methods: correlation based, descriptor/patch based, variational, deep learning, sparse vs. dense

Illustration: Non-Uniqueness

$$u_2(x + v(x)) = u_1(x)$$

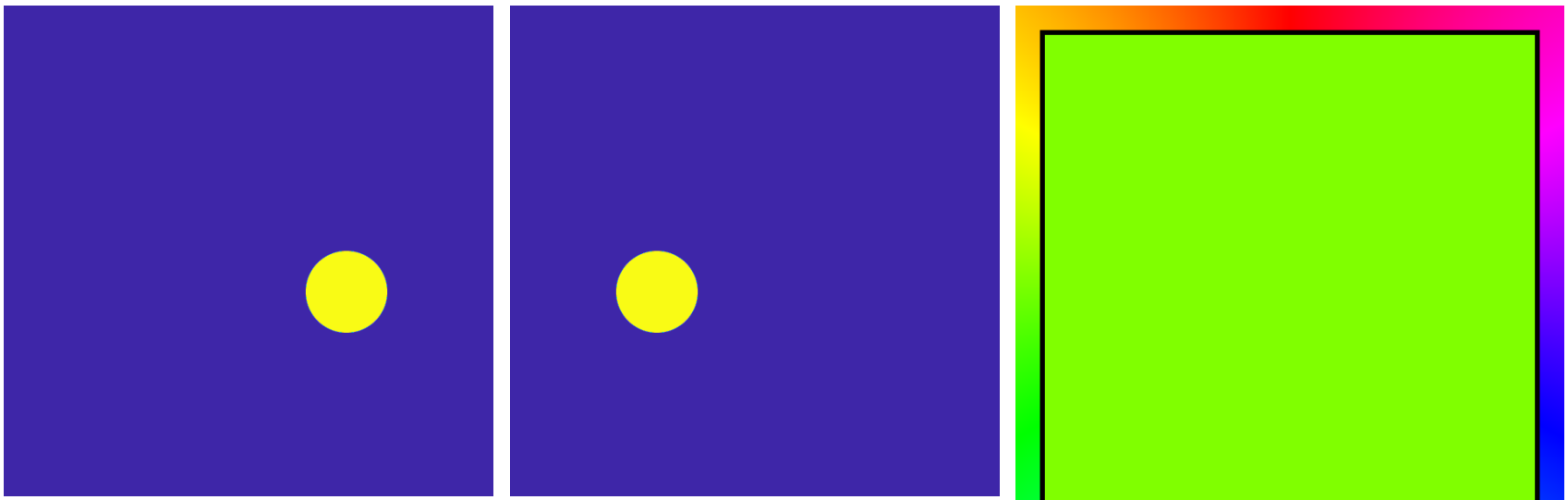

u_1 u_2 v_1

Illustration: Non-Uniqueness

$$u_2(x + v(x)) = u_1(x)$$

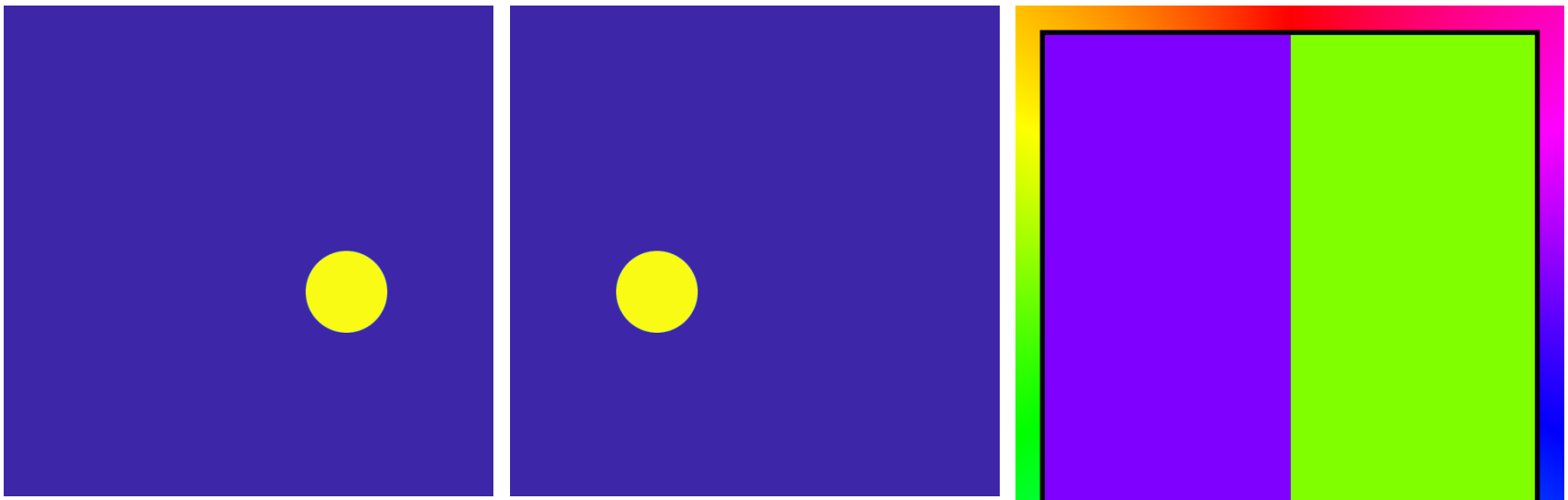

u_1 u_2 v_2

Illustration: Non-Uniqueness

$$u_2(x + v(x)) = u_1(x)$$

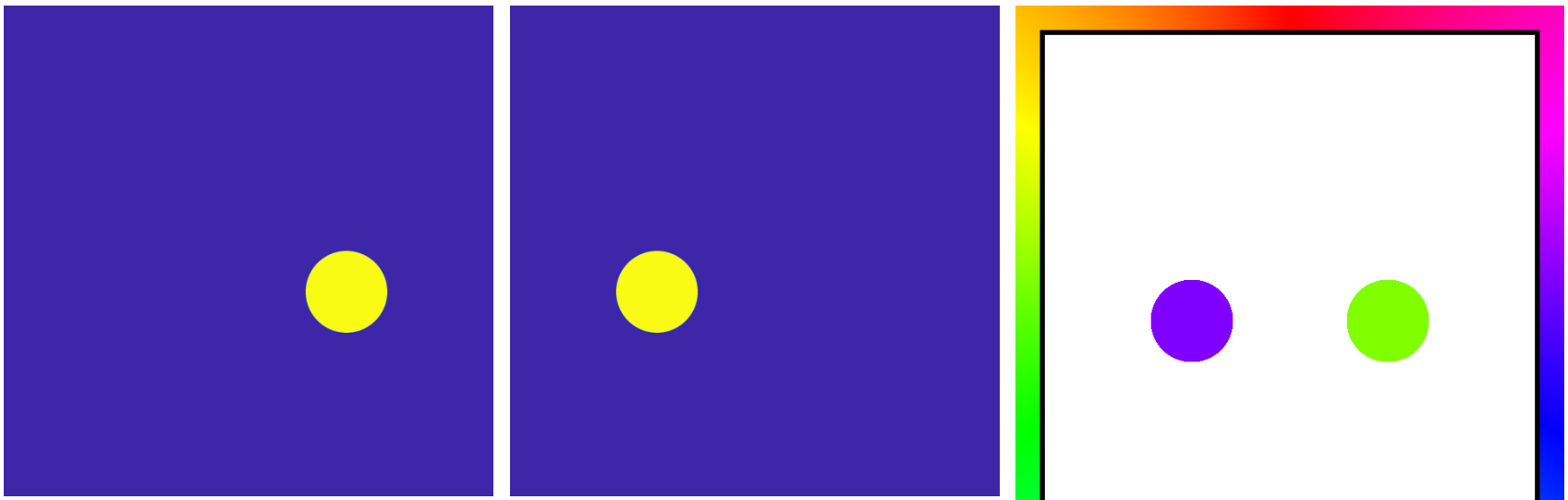

u_1 u_2 v_3

Illustration: Non-Uniqueness

$$u_2(x + v(x)) = u_1(x)$$

u_1

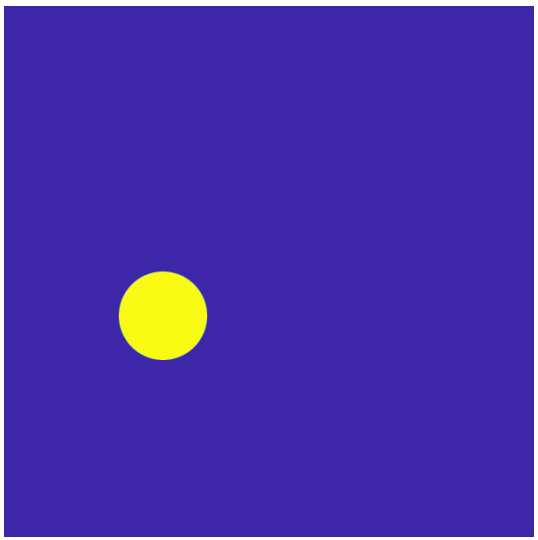

u_2

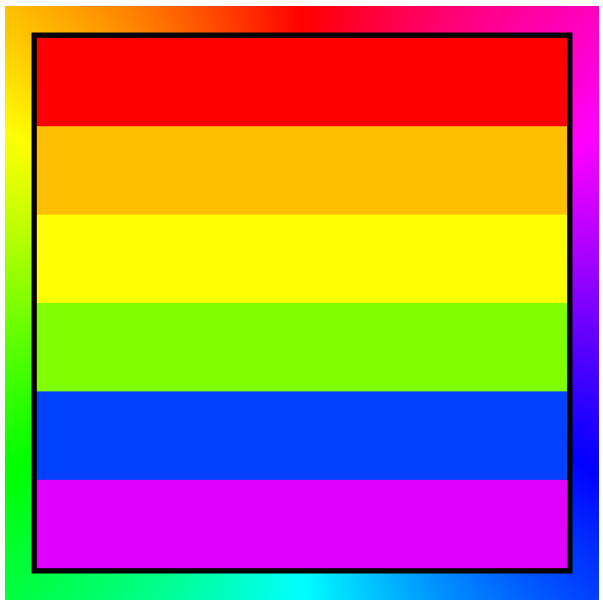

v_4

Alternating Image Reconstruction and Correspondence Analysis

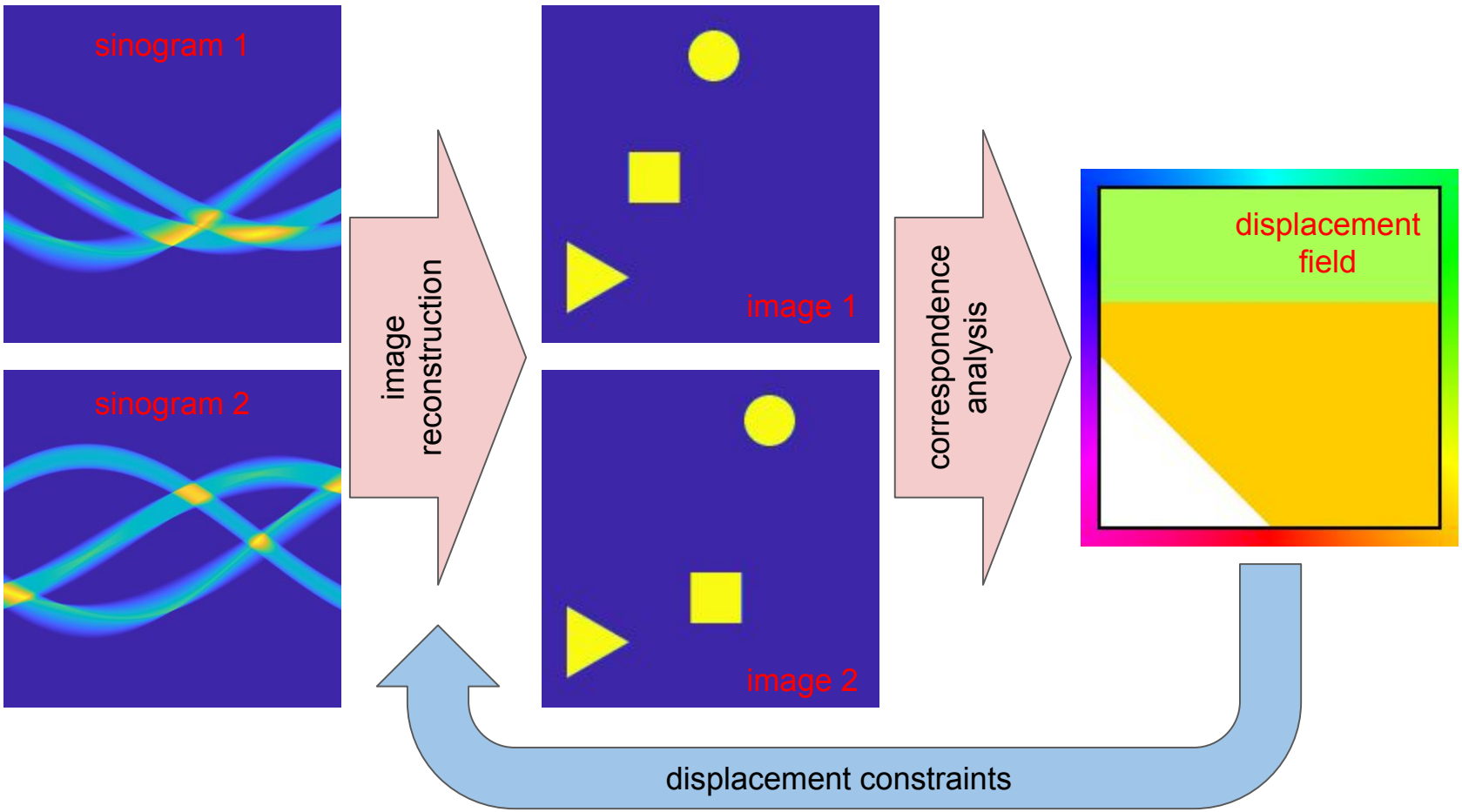

Simultaneous Image Reconstruction and Motion Estimation

$$\min_{u,v} \left(\mathcal{E}(u,v) = \tfrac{1}{2} \sum_{i=1} \| C_i A u_i - f_i \|_2^2 + \alpha \mathcal{R}(u_i) + \beta \mathcal{H}(v_i) + \gamma \mathcal{M}(u,v) \right)$$

$$\mathcal{M}(u,v) := \sum_i \tfrac{1}{p} \, \| u_{i+1}(x + v_i(x)) - u_i(x) \|_p^p$$

- $\mathcal{R}(u_i)$, $\mathcal{H}(v_i)$ typically **convex but non-smooth**, e.g., TV
- $\mathcal{E}(u,v)$ convex in u
- $\mathcal{M}_p^l(u,v)$ convex in $v \implies \mathcal{E}(u,v)$ **bi-convex** in (u,v)

alternating optimization:

$u^{k+1} = \operatorname{argmin}_u \ \mathcal{E}(u, v^k)$ image estimation, convex, non-smooth

$v^{k+1} = \operatorname{argmin}_v \ \mathcal{E}(u^{k+1}, v)$ motion estimation, (non-)convex, non-smooth

Burger, Dirks, Schönlieb, 2018. A Variational Model for Joint Motion Estimation and Image Reconstruction, *SIAM IS.*

Simulation Results: Motion Oracle

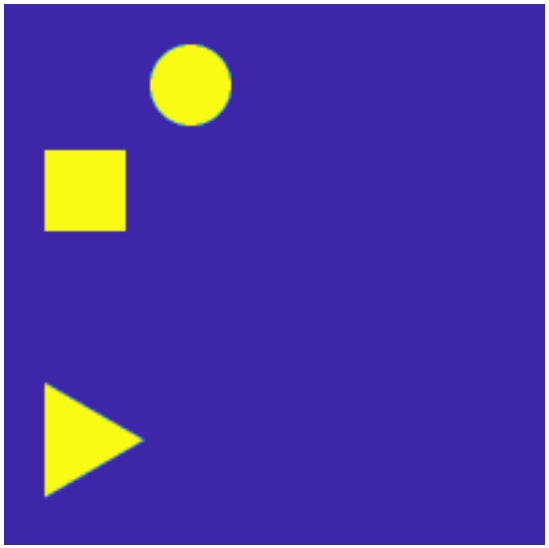
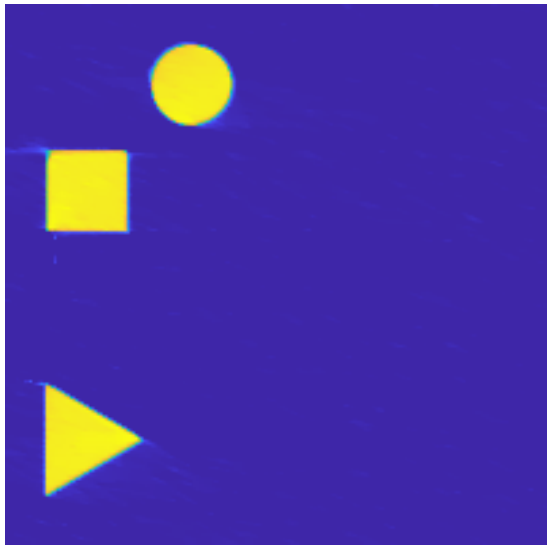
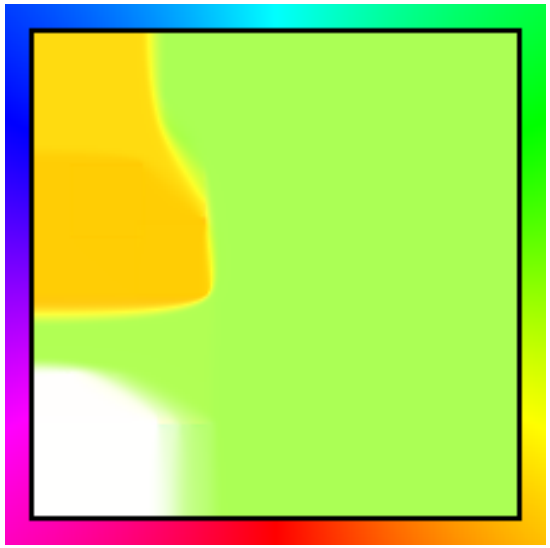

$$\min_{u} \ \frac{1}{2} \sum_{i=1} \| C_i A u_i - f_i \|_2^2 + \alpha TV(u_i) + \beta TV(v_i)$$
$$+ \gamma^2/2 \left(\left\| \mathcal{W}_{v_i^\dagger} u_{i+1} - u_i \right\|_2^2 + \left\| \mathcal{W}_{-v_i^\dagger} u_i - u_{i+1} \right\|_2^2 \right)$$

Simulation Results: Joint Estimation

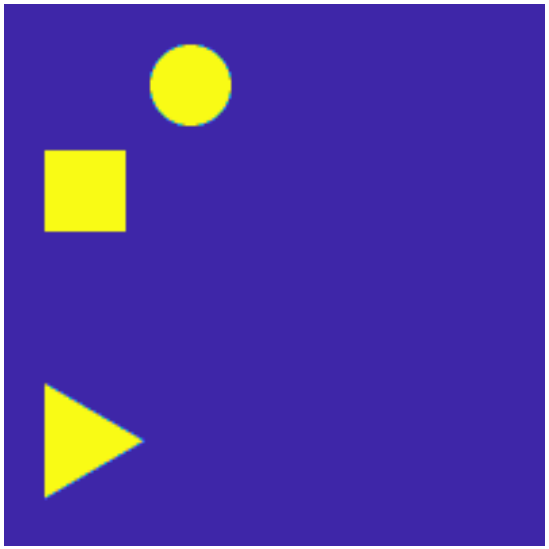
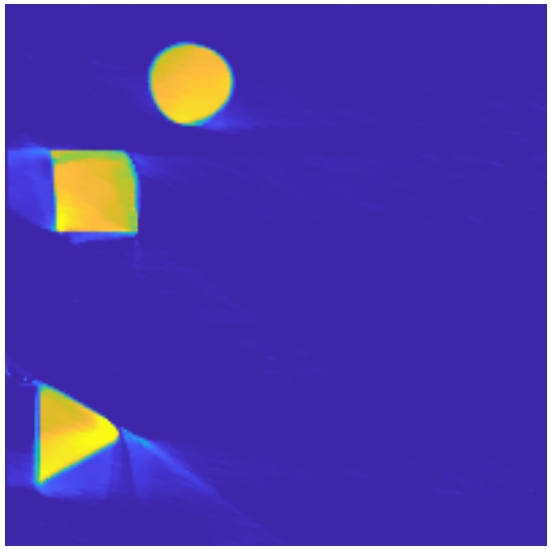
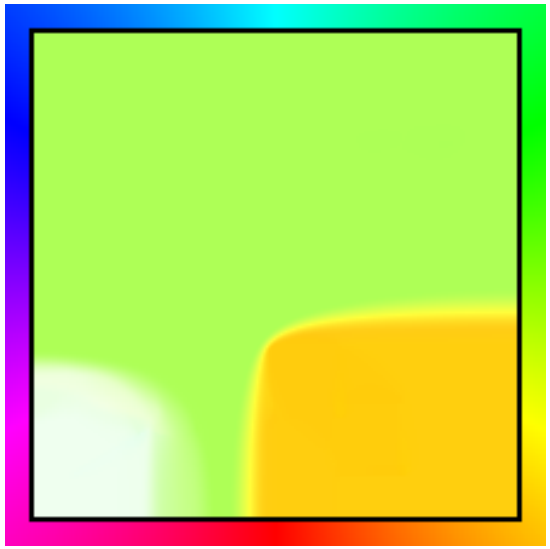

$$\min_{u,v} \ \frac{1}{2} \sum_{i=1} \| C_i A u_i - f_i \|_2^2 + \alpha \, TV(u_i) + \beta \, TV(v_i)$$

$$+ \gamma^2/2 \left(\| \mathcal{W}_{v_i} u_{i+1} - u_i \|_2^2 + \| \mathcal{W}_{-v_i} u_i - u_{i+1} \|_2^2 \right)$$

Lava Lamp Results

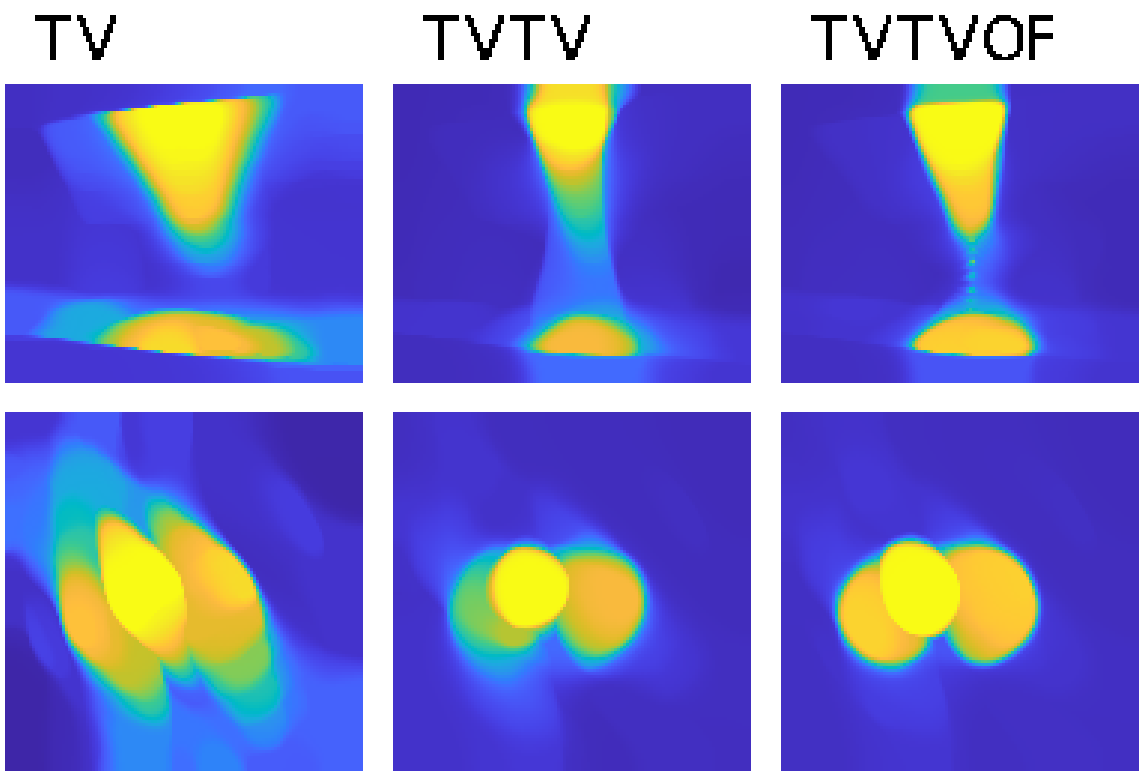

Lava Lamp: Image and Motion Estimation

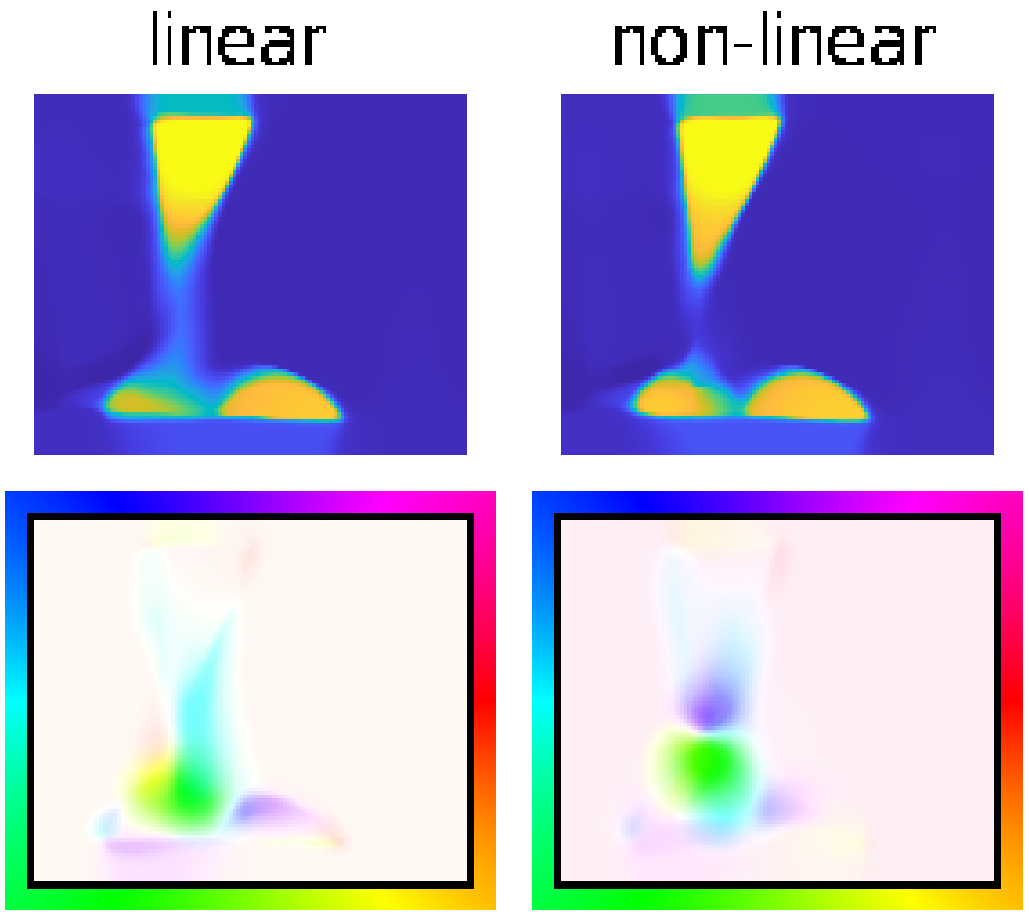

Summary

- dynamic imaging is **hard in both theory and practice**
- **trade-off** between spatial and temporal resolution
- motion estimation (correspondence problem) is tough
- sequential scanning is the worst
- simultaneous image reconstruction and motion estimation
- spatio-temporal regularization via **hidden variable models**
- heavy numerical optimization

CWI

L, Coban, Grass, Lagerwerf, Der Sarkissian, Palenstijn, Batenburg, 202?. Dynamic Tomography of Rapid Deformations with Sequential Scanning, *in preparation.*

L, Huynh, Betcke, Zhang, Beard, Cox, Arridge, 2018. Enhancing Compressed Sensing Photoacoustic Tomography by Simultaneous Motion Estimation, *SIAM Imaging Sciences 11 (4).*

CWI

Thank you for your attention!

L, Coban, Grass, Lagerwerf, Der Sarkissian, Palenstijn, Batenburg, 202?. Dynamic Tomography of Rapid Deformations with Sequential Scanning, *in preparation.*

L, Huynh, Betcke, Zhang, Beard, Cox, Arridge, 2018. Enhancing Compressed Sensing Photoacoustic Tomography by Simultaneous Motion Estimation, *SIAM Imaging Sciences 11 (4).*

Continuous Derivation

Assume intensity $u(x,t)$ constant along $x(t)$ with $\frac{dx}{dt} = \tilde{v}(x,t)$ (velocity):

$$0 = \frac{d}{dt}u(x(t),t) = \frac{\partial u}{\partial t} + \sum_{k=1}^{d} \frac{\partial u}{\partial x_k}\frac{\partial x_k}{\partial t} = \partial_t u + (\nabla u)\cdot\tilde{v}$$

$\rightsquigarrow$ continuity PDE.

Given $u_1(x) := u(x,t_1)$, $u_2(x) := u(x,t_2)$
net displacement/motion field

$$v(x) = \int_{t_1}^{t_2} q(t)dt, \qquad \text{where } q(t) \text{ solves } \frac{d}{dt}q(t) = \tilde{v}(q(t),t), \quad q(t_1) = x$$

optical flow equation:

$$u_2(x + v(x)) = u_1(x) \qquad \text{! underdetermined !}$$

Variational Motion Estimation

regularized motion estimation

$$\min_v \ \mathcal{H}(v) \quad \textit{such that} \quad u_2(x + v(x)) = u_1(x)$$

$$\min_v \ \tfrac{1}{p} \left\| u_2(x + v(x)) - u_1(x) \right\|_p^p + \beta \mathcal{H}(v) \qquad \text{! terribly non-convex !}$$

Variational Motion Estimation

regularized motion estimation

$$\min_v \ \mathcal{H}(v) \quad \textit{such that} \quad u_2(x + v(x)) = u_1(x)$$

$$\min_v \ \tfrac{1}{p} \left\| u_2(x + v(x)) - u_1(x) \right\|_p^p + \beta \mathcal{H}(v) \qquad \text{! terribly non-convex !}$$

small displacements around $\bar{v}(x)$:

$$u_2(x + v(x)) \approx \bar{u}_2(x) + (\nabla \bar{u}_2(x)) \cdot (v(x) - \bar{v}(x))$$

$$\bar{u}_2(x) := u_2(x + \bar{v}(x)) =: \mathcal{W}_{\bar{v}} u_2 \qquad \textbf{(warping)}$$

$$\min_v \ \tfrac{1}{p} \left\| \bar{u}_2 - (\nabla \bar{u}_2) \cdot \bar{v} - u_1 + (\nabla \bar{u}_2) \cdot v \right\|_p^p + \beta \mathcal{H}(v)$$

for $\bar{v} = 0$ we get to backward-discretized PDE back:

$$\min_v \ \tfrac{1}{p} \left\| u_2 - u_1 + (\nabla u_2) \cdot v \right\|_p^p + \beta \mathcal{H}(v)$$

Computational Solution I

linearized problems:

$$\min_v \ \frac{1}{p} \|a \cdot v - f\|_p^p + \beta \mathcal{H}(v)$$

convex but typically non-smooth, e.g. $p = 1$, $\mathcal{H}(v) = TV(v)$

Primal-dual hybrid gradient: too slow convergence in 3D

Alternating directions method of multipliers (ADMM):

- ! more difficult to parameterize
- ! badly conditioned, large-scale least-squares problems
- ! choice of iterative solver crucial, here **AMG-CG**

Chambolle, Pock, 2016. An introduction to continuous optimization for imaging, *Acta Numerica.*

Computational Solution II

$$\min_v \ \frac{1}{p} \|u_2(x + v(x)) - u_1(x)\|_p^p + \beta \mathcal{H}(v)$$

coarse-to-fine scheme:

- successive smoothing & down-sampling of u_2, u_1
- successive solution of linearized problems on each level
- upsampling of solution and aux variables to finer level
- optional: add line search

Brox, Bruhn, Papenberg, Weickert, 2004. High Accuracy Optical Flow Estimation Based on a Theory for Warping, *ECCV 2004.*

Illustration Small Displacements

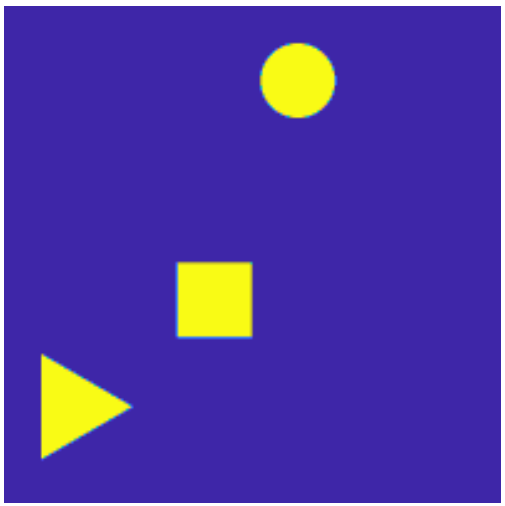

u_1

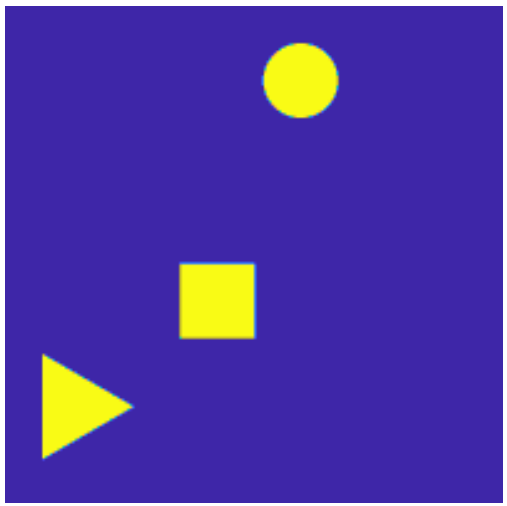

u_2

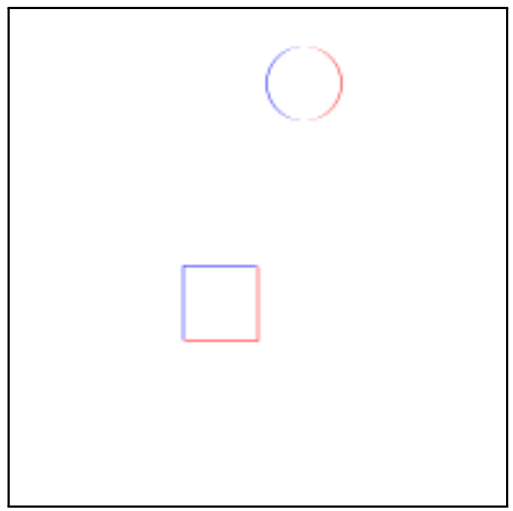

$u_2 - u_1$

Illustration Small Displacements

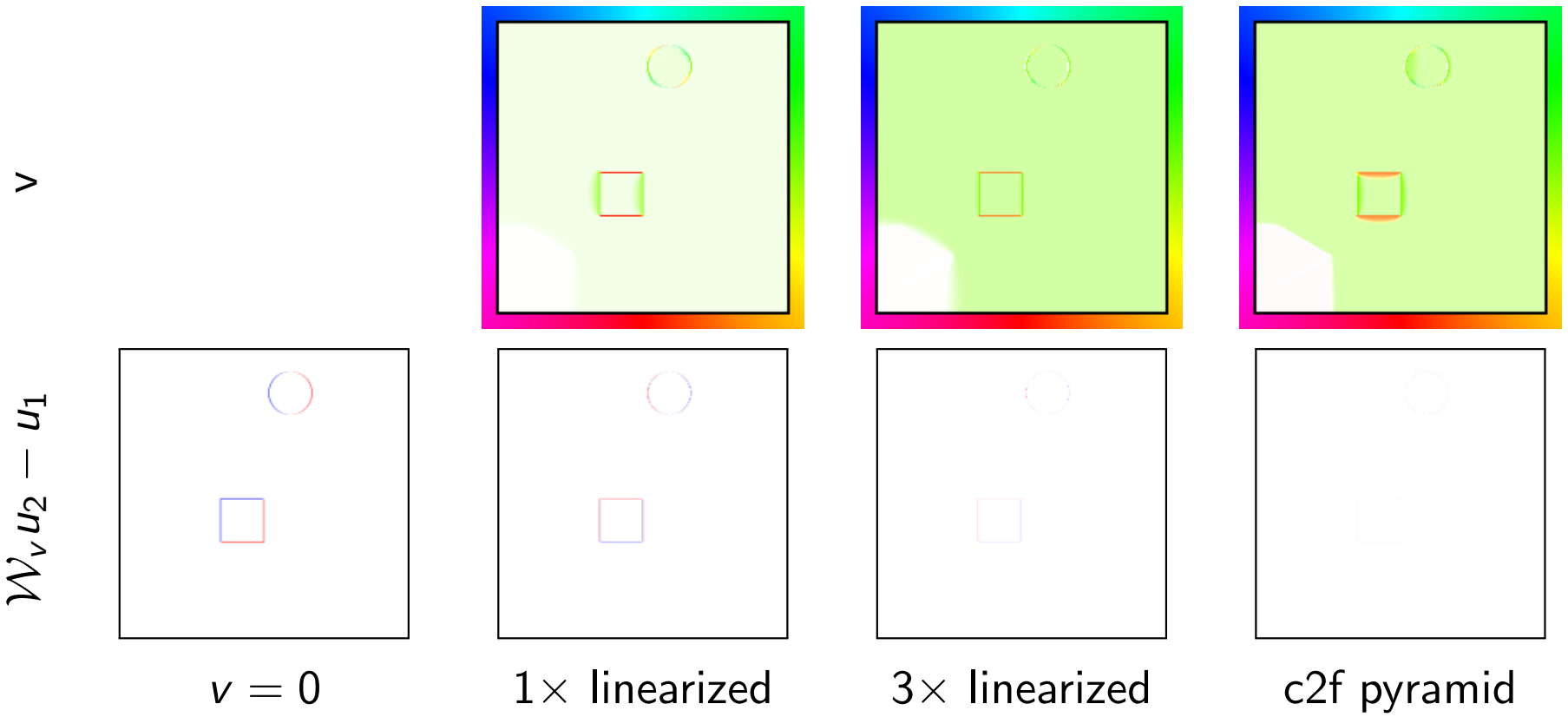

$\|\mathcal{W}_v u_2 - u_1\|$:

5.7	3.3	1.1	0.2

Illustration Medium Displacements

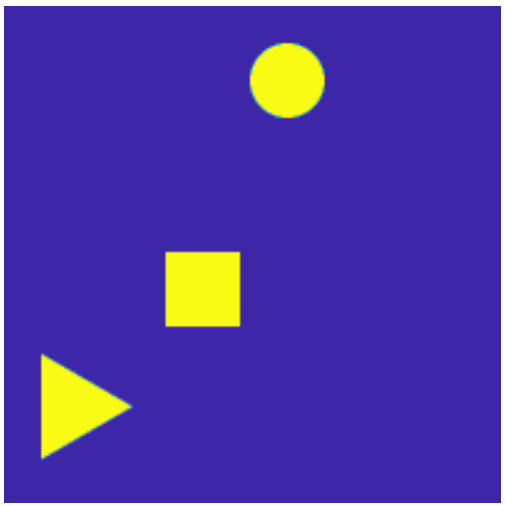

u_1

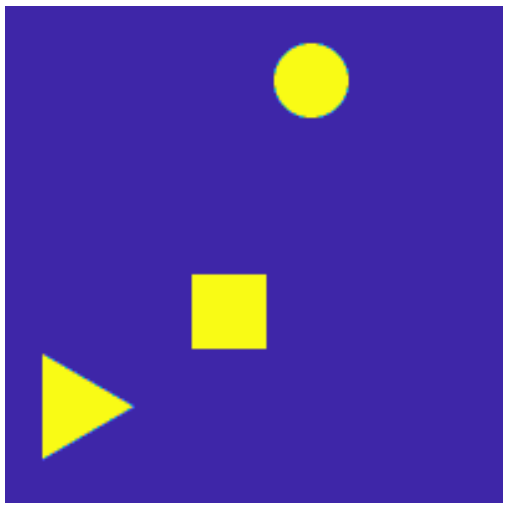

u_2

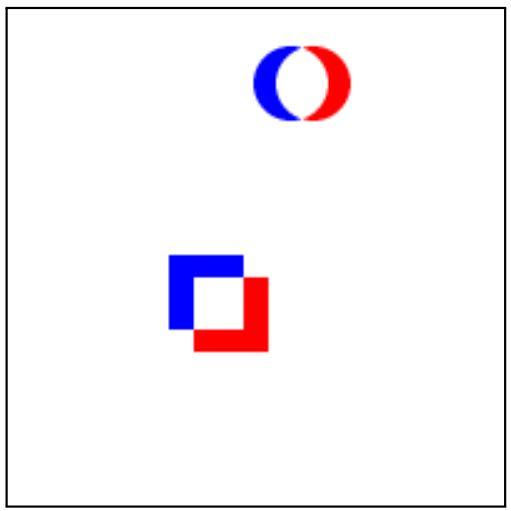

$u_2 - u_1$

Illustration Medium Displacements

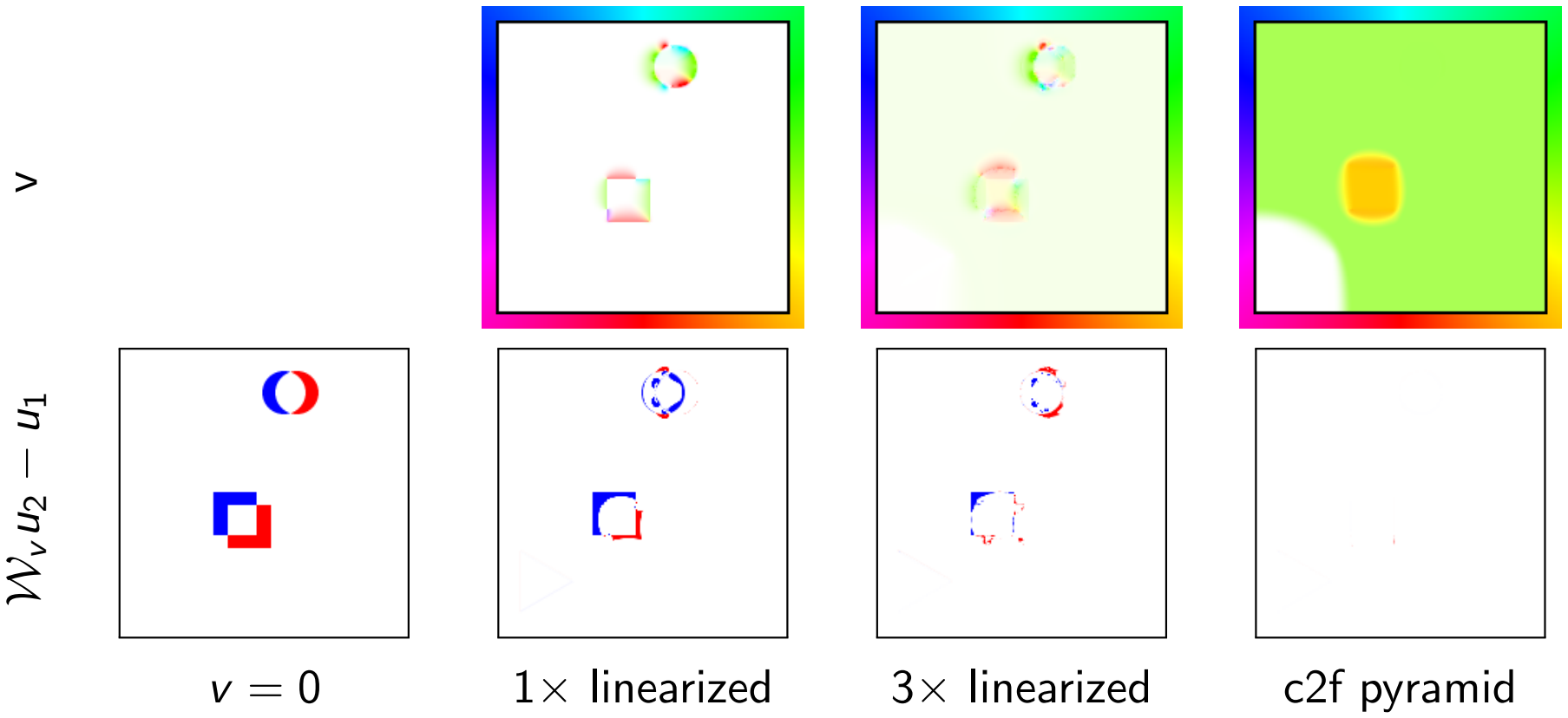

Illustration Large Displacements

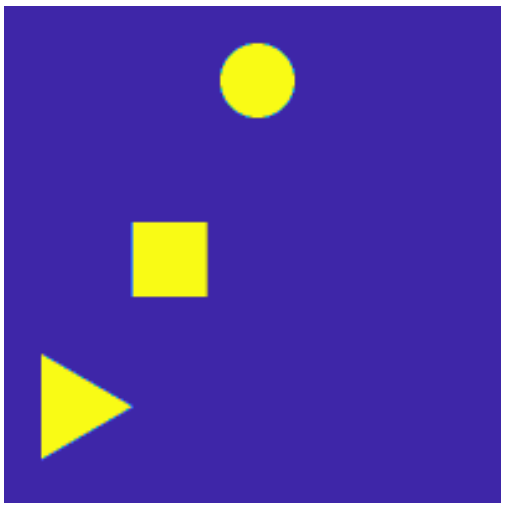

u_1

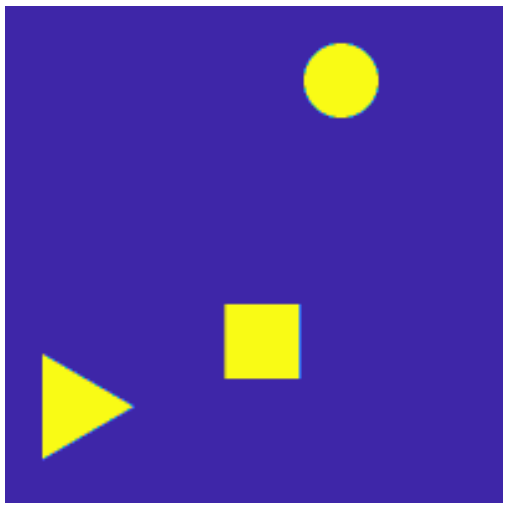

u_2

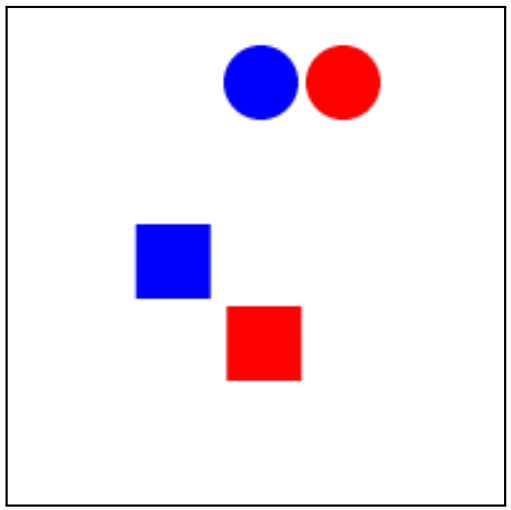

$u_2 - u_1$

Illustration Large Displacements

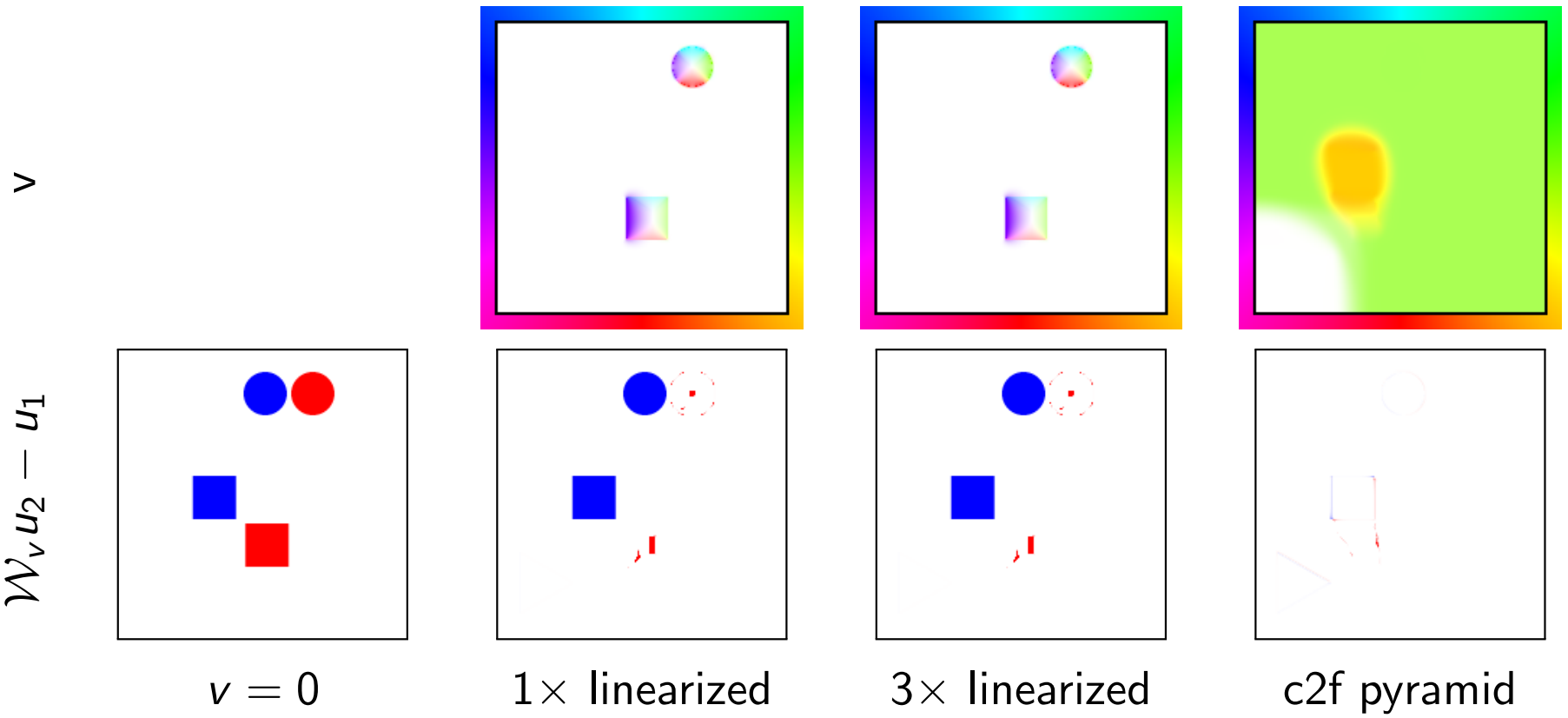

$\|\mathcal{W}_v u_2 - u_1\|$:

$v = 0$	1× linearized	3× linearized	c2f pyramid
56.3	40.9	40.9	2.7

Illustration Pyramid Schemes

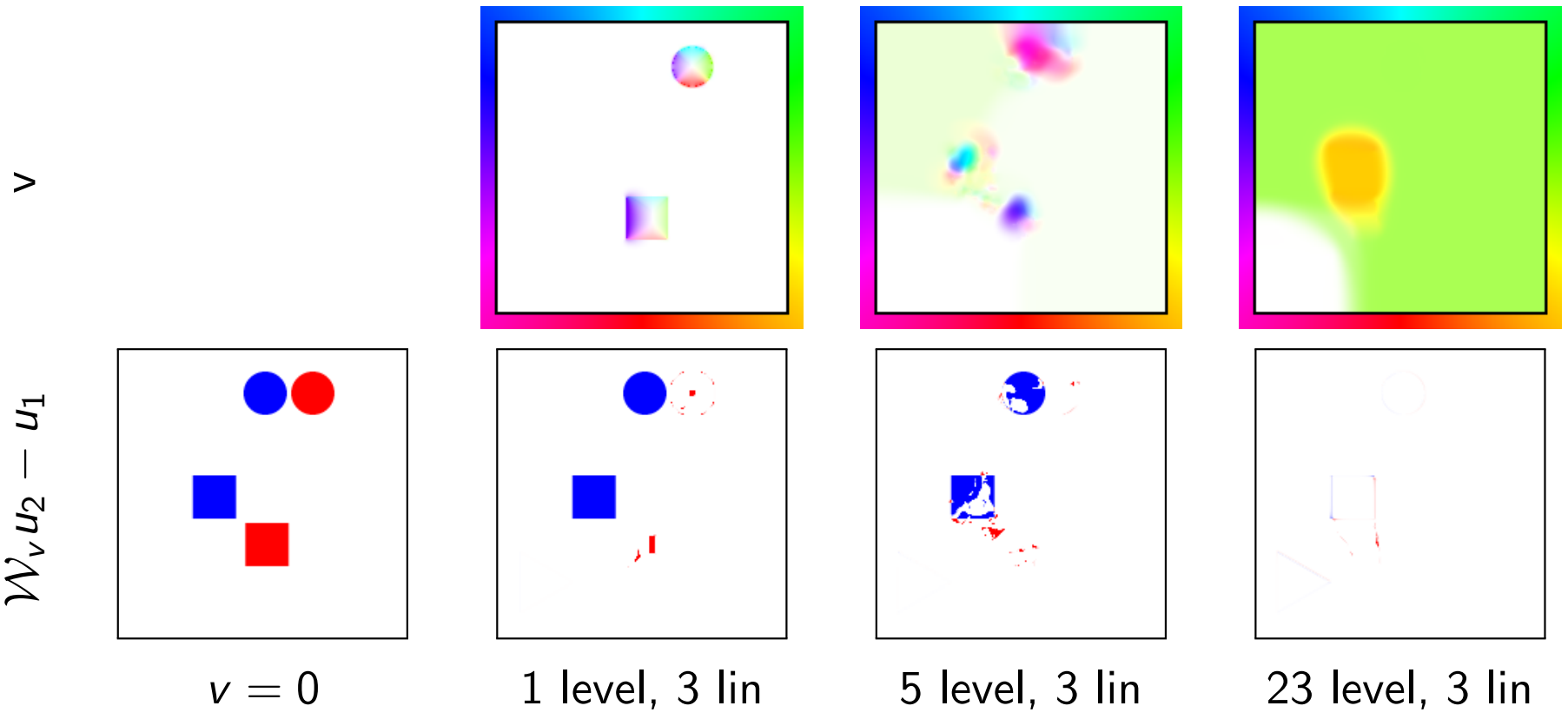

$\|\mathcal{W}_v u_2 - u_1\|$:

56.3	40.9	33.7	2.7

Illustration Symmetric OF

$$v^{fwd} = \underset{v}{\operatorname{argmin}} \ \tfrac{1}{2} \left\| u_2(x+v) - u_1(x) \right\|_2^2 + \beta \mathcal{H}(v)$$

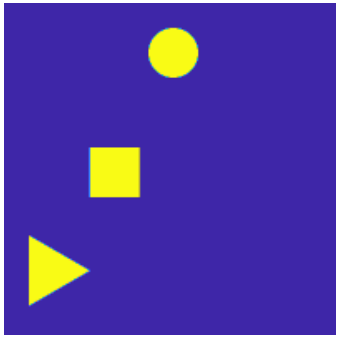

u_1

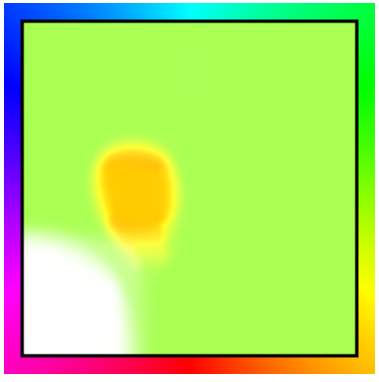

v^{fwd}

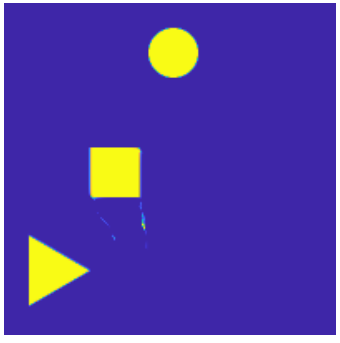

$u_2(x + v^{fwd})$

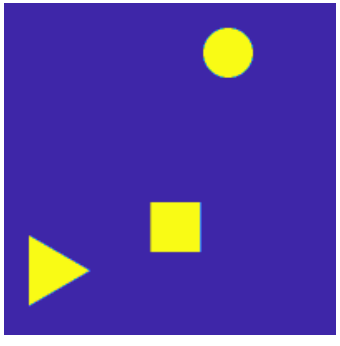

u_2

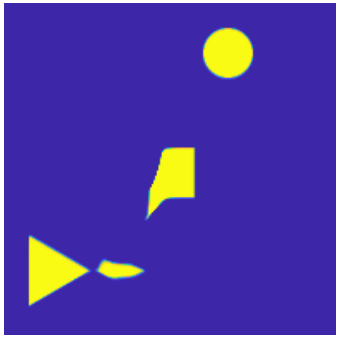

$u_1(x - v^{fwd})$

Illustration Symmetric OF

$$v^{fwd} = \underset{v}{\operatorname{argmin}} \ \tfrac{1}{2} \left\| u_2(x+v) - u_1(x) \right\|_2^2 + \beta \mathcal{H}(v)$$

$$v^{sym} = \underset{v}{\operatorname{argmin}} \ \tfrac{1}{4} \left\| u_2(x+v) - u_1(x) \right\|_2^2 + \tfrac{1}{4} \left\| u_1(x-v) - u_2(x) \right\|_2^2 + \beta \mathcal{H}(v)$$

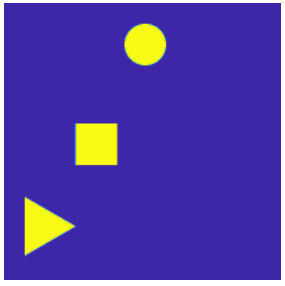

u_1

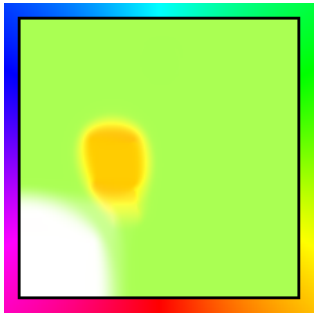

v^{fwd}

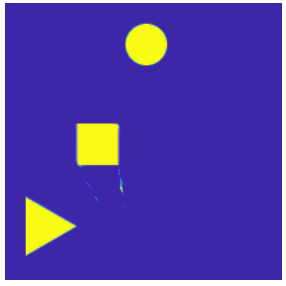

$u_2(x + v^{fwd})$

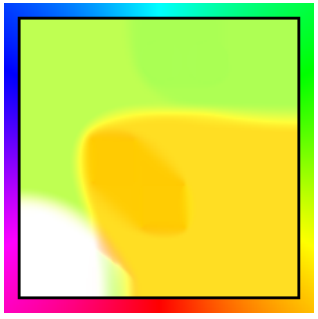

v^{sym}

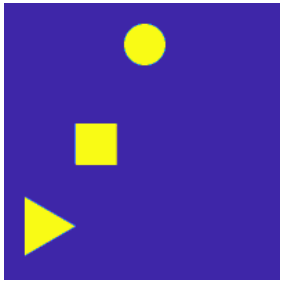

$u_2(x + v^{sym})$

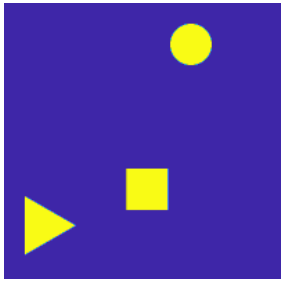

u_2

$u_1(x - v^{fwd})$

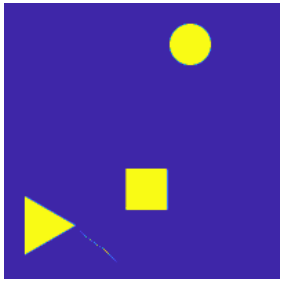

$u_1(x - v^{sym})$